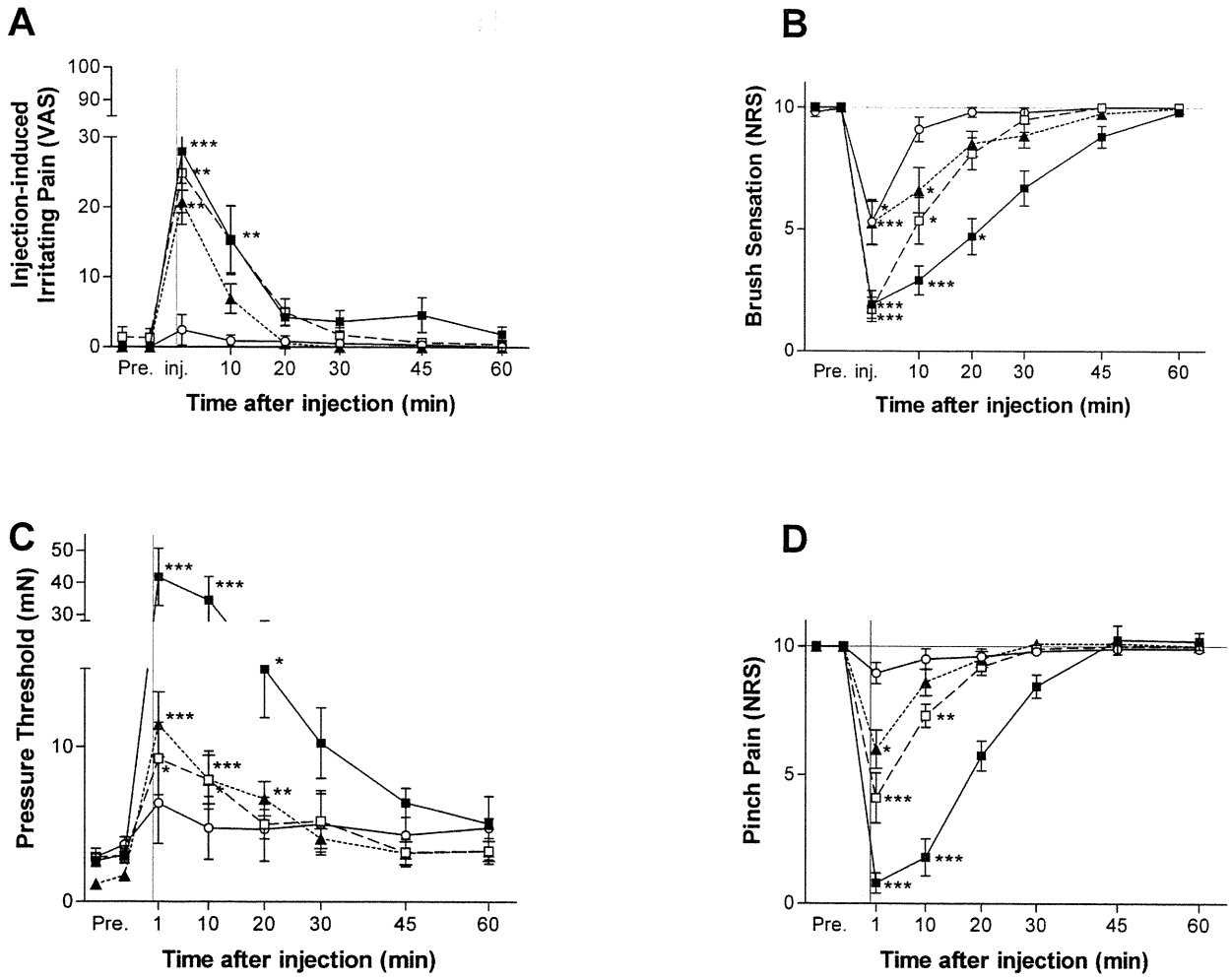

Figure 2
Time course of changes in effect of magnesium ion on pain and sensations. Fifteen volunteers were intradermally injected with 0.5 M $MgSO_4$ (black square), 0.05 M $MgSO_4$ (white square), 0.05 M $MgCl_2$ (black triangle), or saline (white circle). Each volunteer was injected with three kinds of magnesium solution at intervals of at least one week. Local spontaneous pain (A) was reported by visual analogue scale (VAS), Tactile sensation (B) and pinch pain intensity (D) were reported by a numerical rating score (NRS). When $MgSO_4$ and $MgCl_2$ solutions were injected, transient irritating pain and local hypesthesia to mechanical stimuli appeared at the injection site. *$p < 0.05$ vs. control; **$p < 0.01$ vs. control, ***$p < 0.001$ vs. control. As values were similar among these three saline injections, we have put the representative data herein.

modal receptors, Sato et al. showed that reduction of extracellular Ca^{2+} augmented the neuronal responses caused by hypertonic saline and high K solutions and also showed the augmented neuronal responses returned to control levels by an addition of Mg^{2+}, which suggests Mg^{2+} has a similar membrane-stabilizing effect on nerves to Ca^{2+}[11].

In addition, Chaban indicated that NMDA receptors on the periphery are involved in the transmission of noxious mechanical stimulation [12]. Only little attention has being paid so far to the functional importance of the peripherally-distributed NMDA receptors [7]. In a previous study, Ushida et al. evaluated the importance of mechanical stimulation by studying the relationship between magnesium ions and peripheral NMDA receptors [13]. It was found that injection of MK-801, an NMDA receptor antagonist, into the peripheral skin of rats produces inhibition of the sensations induced by innocuous and noxious stimulation.

Paradoxically, present results have shown that local administration of Mg^{2+} induces heat hyperalgesia, but mechanical hypesthesia at the injection site. Only a few

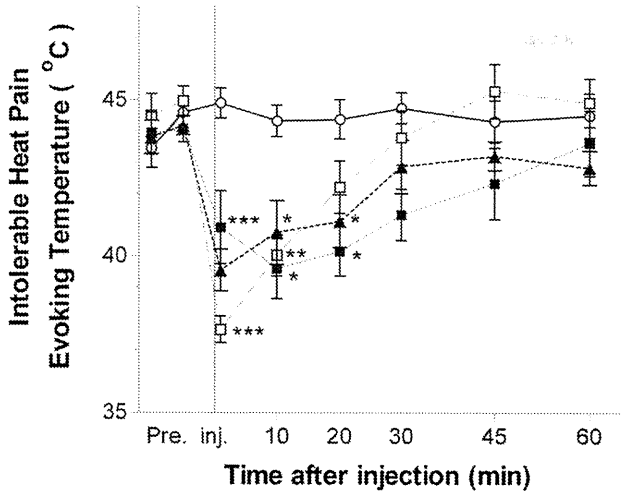

Figure 3
Time course of changes in intolerable heat pain evoking temperature after intradermal injection of magnesium solution. Fifteen volunteers were intradermally injected with 0.5 M $MgSO_4$ (black square), 0.05 M $MgSO_4$ (white square), 0.05 M $MgCl_2$ (black triangle), or saline (white circle). Each volunteer was injected with three kinds of magnesium solution at intervals of at least one week. Intolerant heat pain temperature was decreased at least 10 min following local administration of Mg^{2+}. *p < 0.05 vs. control; **p < 0.01 vs. control, ***p < 0.001 vs. control. As values were similar among these three saline injections, we have put the representative data herein.

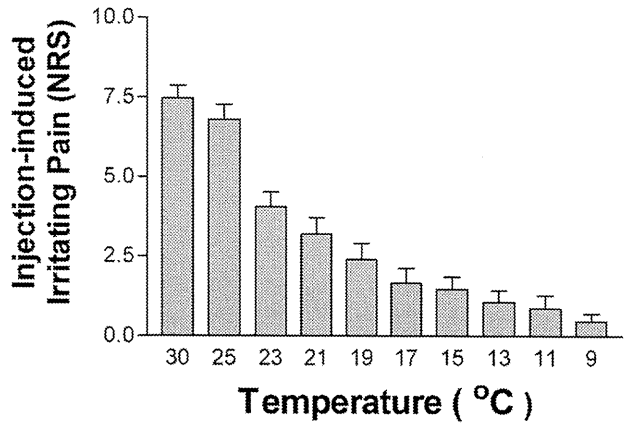

Figure 4
Changes in experienced pain intensity by local cooling. After intradermal administration of 0.5 M $MgSO_4$, Peltier probe was directly attached to the injection site. Pain intensity was substantially attenuated according to the cooling temperature. (n = 15)

researchers have paid attention to changes in Mg^{2+} -induced thermal sensations. Oral administration [14] and intrathecal injection [15] of magnesium sulphate are reported to improve heat hyperalgesia in animal models of neuropathic pain. On the other hand, Mikkelsen et al. reported that intravenous infusion of magnesium had no analgesic effect on thermal sensation in hyperalgesic skin but produced a decreased heat detection threshold and increased pain caused by 1 min long 45°C heat stimulation [9]. Since we could not find any sensory changes outside of wheals, peripheral mechanisms were suggested to explain magnesium-induced heat hyperalgesia.

Recently, transient receptor potential cation channel, subfamily V, member 1 (TRPV1), a heat-sensitive ion channel, has been discovered [16] and the role of this channel may be implicated in Mg^{2+}-induced heat hyperalgesia observed in our study. Indeed, Ahern et al. showed extracellular cations such as Na^+, Ca^{2+}, Mg^{2+} modulate/open the gates of TRPV1 channel by in vitro whole cell and single channel patch-clamp recording studies [17]. In addition to this direct mechanism, several neuropeptides and inflammatory mediators may be implicated in the enhanced activation of TRPV1. The flare formation observed at the injection site suggesting existence of axonal reflex-induced neuropeptide (SP, CGRP, etc) release from sensory nerve endings and released SP may result in sensitizing TRPV1 via activation of NK1, a SP receptor [18]. Also these inflammatory processes may activate the production of bradykinin (BK), a novel algesic substance. Increased extracellular concentration of BK results in sensitization and activates TRPV1 currents via PLC, PKC, and lipoxygenase-derived products [19-21].

These previous studies suggest that TRPV1 may be implicated in Mg^{2+} -induced hyperalgesia. Since cooling is known to desensitize local TRPV1, attenuation of Mg^{2+} -induced irritating pain by local cooling observed in our present study may also be explained by this mechanism.

Recently, types of thermal-sensing receptors such as TRPM8 (Transient receptor potential cation channel, subfamily M, member 8: cool receptor), TRPA1 (transient receptor potential cation channel, member A1: cold receptor), etc. have been discovered after TRPV1 and have been widely investigated [22,23]. In clinical settings, various types of diseases and patients possess the symptoms of thermal (heat, cold) hyperalgesia. However, it has been problematic under such settings to specify the underlying pathological mechanisms in these patients. Presumably, expression or activation of these recently discovered thermal receptors may play a key role in thermal pain and further translational research is necessary for the understanding and treatment of these intractable pain syndromes.

Conclusion

Intradermal administration of magnesium ions locally affected sensory systems and produced spontaneous pain, hypesthesia to both noxious and innocuous mechanical stimuli, and decreased the heat pain threshold. Activation of TRPV1 channel is the suggested mechanism for the development of heat hyperalgesia.

Abbreviations

MS: magnesium sulphate; MC: magnesium chloride; NMDA: N-methyl-D-aspartate; TRPV1: transient receptor potential cation channel, subfamily V, member 1; SP: substance P; CGRP: calcitonin gene-related peptide; NK-1: neurokinin 1; BK: bradykinin; PLC: phospholipase C; PKC: protein kinase C; TRPM8: transient receptor potential cation channel, subfamily M, member 8; TRPA1: transient receptor potential cation channel, member A1

Competing interests

The authors declare that they have no competing interests.

Authors' contributions

TU conceived of the study, participated in its study, and conducted all experiments. OI, KS (Shimo) and TT conducted the acquisition of data. MI and TI performed the statistical analysis. YAP, MN and KS (Suetomi) helped to draft the manuscript. All authors read and approved the final manuscript.

Acknowledgements

The authors would like to express their gratitude to Professor T. Tani and Dr. J. Sato for their invaluable comments on the manuscript and to Ms. Taki for technical assistance.

References

1. Fawcett WJ, Haxby EJ, Male DA: **Magnesium: physiology and pharmacology.** *Br J Anaesth* 1999, **83**:302-320.
2. Frankenhaeuser B, Hodgkin AL: **The action of calcium on the electrical properties of squid axons.** *J Physiol* 1957, **137**:218-244.
3. Hubbard JI, Jones SF, Landau EM: **On the mechanism by which calcium and magnesium affect the release of transmitter by nerve impulses.** *J Physiol* 1968, **196**:75-86.
4. Gean PW, Shinnick-Gallagher P: **Epileptiform activity induced by magnesium-free solution in slices of rat amygdala: antagonism by N-methyl-D-aspartate receptor antagonists.** *Neuropharmacology* 1988, **27**:557-562.
5. Coggeshall RE, Carlton SM: **Ultrastructural analysis of NMDA, AMPA, and kainate receptors on unmyelinated and myelinated axons in the periphery.** *J Comp Neurol* 1998, **391**:78-86.
6. Carlton SM, Coggeshall RE: **Inflammation-induced changes in peripheral glutamate receptor populations.** *Brain Res* 1999, **820**:63-70.
7. Iwatsu O, Ushida T, Tani T, Nada Bashir L, Yamamoto H: **Peripheral Administration of Magnesium Sulfate and Ketamine Hydrochloride Produces Hypesthesia to Mechanical Stimuli in Humans.** *Journal of health science* 2002, **48**:69-72.
8. Dube L, Granry JC: **The therapeutic use of magnesium in anesthesiology, intensive care and emergency medicine: a review.** *Can J Anaesth* 2003, **50**:732-746.
9. Mikkelsen S, Dirks J, Fabricius P, Petersen KL, Rowbotham MC, Dahl JB: **Effect of intravenous magnesium on pain and secondary hyperalgesia associated with the heat/capsaicin sensitization model in healthy volunteers.** *Br J Anaesth* 2001, **86**:871-873.
10. Hahin R, Campbell DT: **Simple shifts in the voltage dependence of sodium channel gating caused by divalent cations.** *J Gen Physiol* 1983, **82**:785-805.
11. Sato J, Mizumura K, Kumazawa T: **Effects of ionic calcium on the responses of canine testicular polymodal receptors to algesic substances.** *J Neurophysiol* 1989, **62**:119-125.
12. Chaban VV, Li H, Ennes HS, Nie J, Mayer EA, McRoberts JA: **N-methyl-D-aspartate receptors enhance mechanical responses and voltage-dependent Ca^{2+} channels in rat dorsal root ganglia neurons through protein kinase C.** *Neuroscience* 2004, **128**:347-357.
13. Ushida T, Tani T, Kawasaki M, Iwatsu O, Yamamoto H: **Peripheral administration of an N-methyl-D-aspartate receptor antagonist (MK-801) changes dorsal horn neuronal responses in rats.** *Neurosci Lett* 1999, **260**:89-92.
14. Hasanein P, Parviz M, Keshavarz M, Javanmardi K, Mansoori M, Soltani N: **Oral magnesium administration prevents thermal hyperalgesia induced by diabetes in rats.** *Diabetes Res Clin Pract* 2006, **73**:17-22.
15. Xiao WH, Bennett GJ: **Magnesium suppresses neuropathic pain responses in rats via a spinal site of action.** *Brain Res* 1994, **666**:168-172.
16. Tominaga M, Caterina MJ, Malmberg AB, Rosen TA, Gilbert H, Skinner K, Raumann BE, Basbaum AI, Julius D: **The cloned capsaicin receptor integrates multiple pain-producing stimuli.** *Neuron* 1998, **21**:531-543.
17. Ahern GP, Brooks IM, Miyares RL, Wang XB: **Extracellular cations sensitize and gate capsaicin receptor TRPV1 modulating pain signaling.** *J Neurosci* 2005, **25**:5109-5116.
18. Zhang H, Cang CL, Kawasaki Y, Liang LL, Zhang YQ, Ji RR, Zhao ZQ: **Neurokinin-1 receptor enhances TRPV1 activity in primary sensory neurons via PKCepsilon: a novel pathway for heat hyperalgesia.** *J Neurosci* 2007, **27**:12067-12077.
19. Premkumar LS, Ahern GP: **Induction of vanilloid receptor channel activity by protein kinase C.** *Nature* 2000, **408**:985-990.
20. Chuang HH, Prescott ED, Kong H, Shields S, Jordt SE, Basbaum AI, Chao MV, Julius D: **Bradykinin and nerve growth factor release the capsaicin receptor from PtdIns(4,5)P2-mediated inhibition.** *Nature* 2001, **411**:957-962.
21. Shin J, Cho H, Hwang SW, Jung J, Shin CY, Lee SY, Kim SH, Lee MG, Choi YH, Kim J, Haber NA, Reichling DB, Khasar S, Levine JD, Uhtaek Oh: **Bradykinin-12-lipoxygenase-VR1 signaling pathway for inflammatory hyperalgesia.** *Proc Natl Acad Sci USA* 2002, **99**:10150-10155.
22. Obata K, Katsura H, Mizushima T, Yamanaka H, Kobayashi K, Dai Y, Fukuoka T, Tokunaga A, Tominaga M, Noguchi K: **TRPA1 induced in sensory neurons contributes to cold hyperalgesia after inflammation and nerve injury.** *J Clin Invest* 2005, **115**:2393-2401.
23. Tominaga M, Caterina MJ: **Thermosensation and pain.** *J Neurobiol* 2004, **61**:3-12.

Hindawi Publishing Corporation
Evidence-Based Complementary and Alternative Medicine
Volume 2011, Article ID 543291, 6 pages
doi:10.1155/2011/543291

Research Article

Comparative Effects of Acupressure at Local and Distal Acupuncture Points on Pain Conditions and Autonomic Function in Females with Chronic Neck Pain

Takako Matsubara,[1,2] Young-Chang P. Arai,[2] Yukiko Shiro,[3] Kazuhiro Shimo,[2] Makoto Nishihara,[2] Jun Sato,[4] and Takahiro Ushida[2]

[1] *Department of Rehabilitation, Faculty of Health Sciences, Nihon Fukushi University, 26-2 Higashihaemicho, Handa, Aichi 475-0012, Japan*
[2] *Multidisciplinary Pain Centre, School of Medicine, Aichi Medical University, Aichi 480-1195, Japan*
[3] *Department of Rehabilitation, Faculty of Health Sciences, Nagoya Gakuin University, Aichi 480-1298, Japan*
[4] *Futuristic Environmental Simulation Center, Research Institute of Environmental Medicine, Nagoya University, Nagoya 464-8601, Japan*

Correspondence should be addressed to Takako Matsubara, matsubar@n-fukushi.ac.jp

Received 7 July 2010; Accepted 2 September 2010

Acupressure on local and distal acupuncture points might result in sedation and relaxation, thereby reducing chronic neck pain. The aim was to investigate the effect of acupressure at local (LP) and distal acupuncture points (DP) in females with chronic neck pain. Thirty-three females were assigned to three groups: the control group did not receive any stimuli, the LP group received acupressure at local acupuncture points, GB 21, SI 14 and SI 15, and the DP group received acupressure at distal acupuncture points, LI 4, LI 10 and LI 11. Verbal rating scale (VRS), Neck Disability Index (NDI), State-Trait Anxiety Inventory (STAI), muscle hardness (MH), salivary alpha-amylase (sAA) activity, heart rate (HR), heart rate variability (HRV) values and satisfaction due to acupressure were assessed. VRS, NDI, STAI and MH values decreased after acupressure in the LP and the DP group. HR decreased and the power of high frequency (HF) component of HRV increased after acupressure in only the LP group. Although acupressure on not only the LP but also the DP significantly improved pain conditions, acupressure on only the LP affected the autonomic nervous system while acupuncture points per se have different physical effects according to location.

1. Introduction

Chronic neck pain is a very common symptom especially in females. In general, neck pain is felt as a dull pain, stiffness, or discomfort along the trapezius muscles and the muscles around the scapulae [1]. Common treatment for chronic neck pain consists of medication, trigger point injection, massage, and other physical therapies and patient education [2]. Massage therapy applied on the tender points is popular in patients with chronic neck pain and provides the patients not only with comfort during and immediately after it but also with various side effects such as discomfort/soreness, tiredness/fatigue, and headache afterwards [3]. Recently, alternative therapies such as acupuncture and acupressure have been increasingly sought. Acupressure is a noninvasive and safe technique, which is manipulated with the fingers instead of needles on the traditional acupuncture points, and has been shown to be effective in pain relief, sedation, and relaxation [4, 5]. Tender points located on the trapezius muscles are consistent with local acupuncture points such as "*Jianjing*" (GB 21), "*Jianwaishu*" (SI 14), and "*Jianzhongshu*" (SI 15) and are applied to massage therapy in patients with chronic neck pain. On the other hand, distal traditional acupuncture points, "*Hegu*" (LI 4), "*Shousanli*" (LI 10), and "*Quchi*" (LI 11), are contained in the Large Intestine Meridian of Hand-Yangming and are suggested to be the points for improving neck-shoulder-arm disorders in the Chinese/Japanese traditional medicine.

Chronic pain influences the autonomic nervous system. For example, sympathetic hyperactivation was shown in

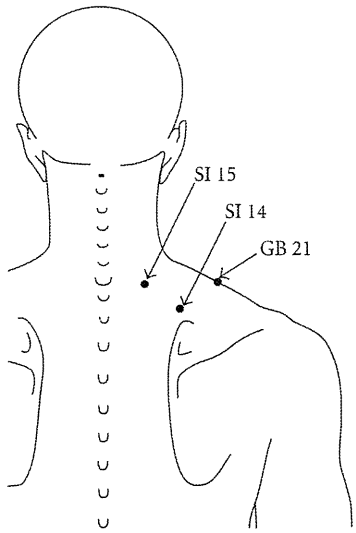

FIGURE 1: Local acupuncture points/tender points. "*Jianjing*" (GB 21) is located at the highest point on the shoulder and at the midpoint of the line which connects the prominent vertebra and the acromion. "*Jianwaishu*" (SI 14) is located directly above the superior angle of scapula, at 5-6 cm lateral from the posterior midline and below the spinous process of the first thoracic vertebra. "*Jianzhongshu*" (SI 15) is located on the back, at 3-4 cm lateral from the posterior midline and below the spinous process of the seventh cervical vertebra.

fibromyalgia (FM) [6], low back pain [7], whiplash associated disorders [8], and migraine [9]. Furthermore, a study showed functional change of the sympathetic nervous system in workers with chronic neck pain [10]. This abnormality in the sympathetic nervous system might generate and sustain chronic pain [11]. Several reports showed that acupuncture and acupressure on the traditional acupuncture points influence the autonomic nervous system [4, 5, 11, 12]. That is, these procedures could modulate the activities of the sympathetic and parasympathetic nerves.

Autonomic nervous function is known to be reflected in heart rate variability. Rhythmic components of HRV can be quantitatively assessed by means of power spectral analysis. HRV is a reliable and noninvasive tool, used to assess autonomic nervous system regulation of the heart [4, 5]. Frequency fluctuations in low frequency of 0.04–0.15 Hz (LF) component of HRV are considered markers of sympathetic and parasympathetic nerve activities, and high frequencies of 0.15–0.4 Hz (HF) component fluctuation of HRV are considered as a marker of parasympathetic nerve activity. Thus, the LF/HF ratio is considered to be an index of sympathetic nerve activity.

We hypothesized that acupressure not only on the tender points/local acupuncture points, "*Jianjing*" (GB 21), "*Jianwaishu*" (SI 14), and "*Jianzhongshu*" (SI 15), but also on the distal acupuncture points, "*Hegu*" (LI 4), "*Shousanli*" (LI 10), and "*Quchi*" (LI 11), could induce sedation, thereby reducing pain, muscle tone, and disability and changing autonomic nervous activity in subjects with chronic neck pain. In the present study, we therefore investigated what effect pressure applied on the local and distal acupuncture points had on the pain conditions and HRV in females with chronic neck pain.

2. Methods

2.1. Subjects. After obtaining approval from the ethics committee of Nihon Fukushi University and written informed consent, 33 female subjects who complained of chronic neck pain participated in the present study. The subjects were randomly allocated to three groups. The exclusion criteria were menstruation, cardiovascular or neurological disease, or administration of sedatives, analgesic, or other medication.

2.2. Group, Administration, and Measurements. Subjects in the local acupuncture point (LP) group received acupressure at three tender points on the neck/shoulder muscles, which were consistent with local acupuncture points, "*Jianjing*" (GB 21), "*Jianwaishu*" (SI 14), and "Jianzhongshu" (SI 15) (Figure 1), subjects in the distal acupuncture point (DP) group received acupressure at three distal acupuncture points, "*Hegu*" (LI 4), "*Shousanli*" (LI 10), and "*Quchi*" (LI 11) (Figure 2), and subjects in the control group did not receive any stimuli.

All measurements were performed during the afternoon hours. Subjects were assessed regarding pain intensity using verbal rating scale (VRS), pain-related disability using Neck Disability Index (NDI), pain-related anxiety using State-Trait Anxiety Inventory-I (STAI-I), muscle hardness (MH) on bilateral trapezius muscles, pain-associated stress using salivary alpha-amylase (sAA) activity, heart rate variability (HRV), and satisfaction using VRS due to acupressure. For the VRS, the intensity of neck pain or stiffness was evaluated on a numerical scale from 0 to 3 (0: no pain, 1: mild pain, 2: moderate pain, and 3: severe pain). NDI, which was published by Vernon in 1991, is the most commonly used and validated scale designed to assess self-rated disability in patients with neck pain and disorder [13]. MH was evaluated using a tissue hardness meter (PEK-1, Imoto Machinery Co. Ltd., Kyoto, Japan) bilaterally on the midpoint between the spinous process of seventh cervical vertebra and the acromion. This point is located on the trapezius muscles, and the tender point of neck pain often lies on this point, which is just the acupuncture point, "*Jianjing*" (GB 21) [1]. sAA was evaluated using a hand-held sAA monitor (CM-2.1, Nipro, Osaka, Japan) [14]. Satisfaction due to acupressure was evaluated on a numerical scale from 0 to 3 (0: no satisfaction, 1: mild satisfaction, 2: moderate satisfaction, and 3: sufficient satisfaction). VRS and STAI-I before, immediately following, and 1 day after receiving the treatment, MH and sAA before and immediately after the treatment, NDI before and 1 day after the treatment, satisfaction immediately following and 1 day after the treatment were sampled.

After the initial assessment, the subjects were allowed to lie comfortably on the bed in a quiet environment for 5 min. Then, the record of the electrocardiogram (ECG) signals for HRV analysis started.

Table 1: Age, weight, VRS, NDI, STAI, MH, sAA, HR, and HRV values at pretreatment for each group.

	C group (n = 11)	LP group (n = 11)	DP group (n = 11)	P value
Age (yr)	34.8 (4.0)	35.5 (6.4)	37.2 (7.0)	.637
Weight (kg)	50.4 (6.8)	52.3 (10.1)	52.2 (4.8)	.643
VRS	1.8 (0.6)	2.1 (0.5)	1.7 (0.8)	.413
NDI	7.9 (3.8)	9.4 (4.4)	7.6 (4.6)	.430
STAI	39.2 (9.5)	44.5 (8.0)	43.2 (6.8)	.772
MH (N)	56.9 (5.0)	57.4 (4.5)	56.2 (5.3)	.507
sAA (kU/l)	38.2 (20.1)	20.0 (9.0)	36.8 (27.9)	.079
HR (bpm)	65.4 (8.7)	65.8 (6.7)	62.3 (14.1)	.941
LF (ms^2)	490.7(409.2)	274.2 (253.3)	494.1 (1050.7)	.084
HF (ms^2)	381.8(338.3)	212.8 (186.7)	764.8 (1045.2)	.587
LF/HF	1.7(1.4)	1.4 (0.8)	1.0 (0.6)	.399

Values expressed as mean (SD).VRS: verbal rating scale. NDI: Neck Disability Index. STAI: State-Trait Anxiety Inventory-I. MH: muscle hardness. sAA: salivary alpha-amylase. HR: heart rate. LF: the power of low-frequency (0.04–0.15 Hz, LF) component of heart rate variability (HRV). HF: the power of high-frequency (0.15–0.4 Hz, HF) component of HRV. LF/HF: LF/HF ratio of HRV.

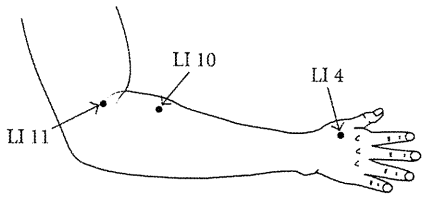

Figure 2: Distal acupuncture point. "*Hegu*" (LI 4) is the most important analgesic point in the body and is intensively stimulated in all painful conditions and is located on the highest point of the adductor pollicis muscle with the thumb and index finger adducted. "*Shousanli*" (LI 10) is located on the radial side of the dorsal surface of the forearm at about 3 cm below the lateral transverse elbow crease and between the extensor carpi radialis longus and brevis. "*Quchi*" (LI 11) is located on the end of the lateral transverse elbow crease at the middle of the connection between the biceps tendon and the lateral epicondylus of the humerus.

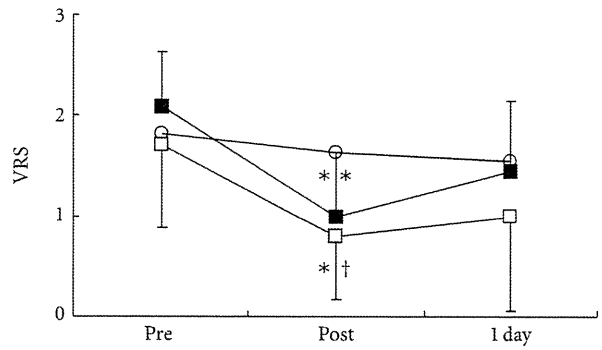

Figure 3: Changes in pain intensity (VRS: verbal rating scale). ○: control group. ■: local acupuncture point (LP) group. □: distal acupuncture point (DP) group. Values are presented as mean. SD represented with error bars in the LP and the DP groups. * significantly different from pre-treatment in the DP group (P < .05). ** significantly different from pretreatment in the LP group (P < .01). † significantly different from control group in the DP group (P < .05).

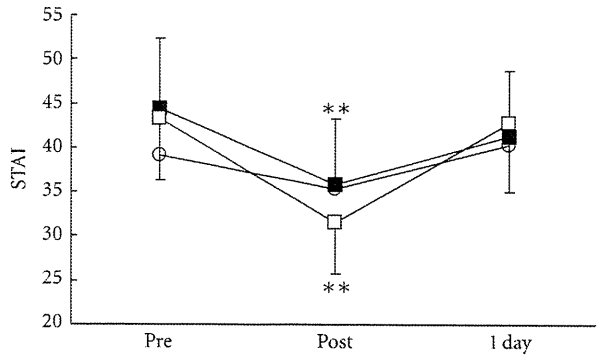

Figure 4: Changes in pain-associated anxiety (STAI-I: State-Trait Anxiety Inventory-I). ○: control group. ■: local acupuncture point (LP) group. □: distal acupuncture point (DP) group. Values are presented as mean. SD represented with error bars in the LP and the DP groups. ** significantly different from pre-treatment in the LP and the DP groups (P < .01).

Ten minutes later, three sets of acupressure by the pulp of the right thumb in a rotary fashion at 20–25 cycles per minute for 30 seconds on each point were administered at the right side of GB 21, SI 14, and SI 15 consecutively and afterwards at the left side of these three points in the LP group. On the other hand, three sets of procedures conducted in the same way as shown in the LP group were administered at the right side of LI 4, LI 10, and LI 11 consecutively and afterwards on the left side of these three points in the DP group. These procedures were applied by the same investigator. Following release of acupressure, the subjects were observed for another 10 minutes. The ECG signals were obtained from a portable ECG (AC301A, GMS, Tokyo, Japan) and transferred to a computer loaded with HRV analysis software (TARAWA/WIN; Suwa Trust, Tokyo, Japan). The R-R intervals (RRIs) were obtained every 10 seconds. The two components of power of the RRI (ms.ms), LF (0.04–0.15 Hz) and HF (0.15–0.5 Hz), were calculated.

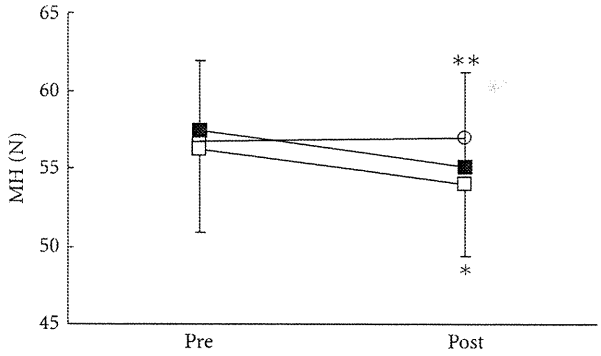

FIGURE 5: Changes in muscle hardness (MH). ○: control group. ■: local acupuncture point (LP) group. □: distal acupuncture point (DP) group. Values are presented as mean. SD represented with error bars in the LP and the DP groups. * significantly different from pre-treatment in the DP group ($P < .05$). ** significantly different from pre-treatment in the LP group ($P < .01$).

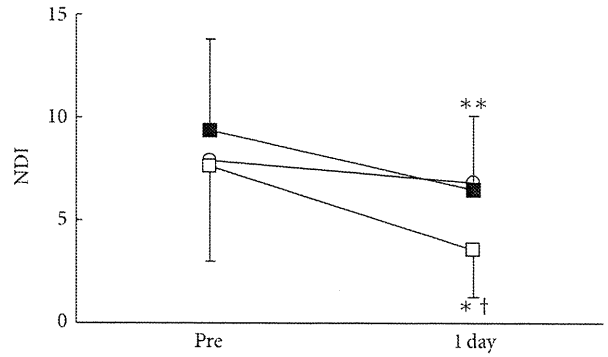

FIGURE 6: Changes in pain-associated disability (NDI:Neck Disability Index). ○: control group. ■: local acupuncture point (LP) group. □: distal acupuncture point (DP) group. Values are presented as mean. SD represented with error bars in the LP and the DP groups. * significantly different from pre-treatment in the DP group ($P < .05$). ** significantly different from pre-treatment in the LP group ($p < .01$). † significantly different from control group in the DP group ($P < .05$).

Heart rate (HR) and the LF and the HF values and the LF/HF ratio of HRV were analyzed. The data of HR and HRV values for 30 seconds at 5 minutes before the beginning of the pressure (pre-treatment) and for 30 seconds at 5 minutes after pressure release (post-treatment) were sampled for subsequent analysis.

2.3. Data Analysis. Data was presented as mean (SD). VRS, STAI-I, MH, NDI, HR, and HRV values were analyzed with Kruskal-Wallis test for intergroup comparison followed by Dunn's Multiple Comparison Test. Satisfaction due to acupressure was analyzed with Mann-Whitney's U test for intergroup comparison on the LP and the DP groups. VRS and STAI-I were analyzed using Friedman test for intragroup comparison followed by Dunn's Multiple Comparison Test. Wilcoxon signed-rank test was used to analyze MH, NDI, HR, and HRV values for intragroup comparison. $P < .05$ was considered as statistically significant.

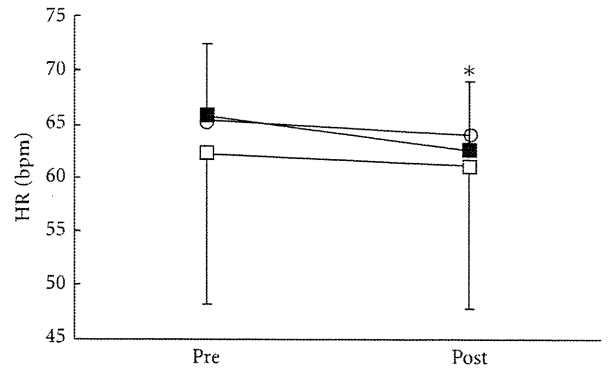

FIGURE 7: Changes in heart rate (HR). ○: control group. ■: local acupuncture point (LP) group. □: distal acupuncture point (DP) group. Values are presented as mean. SD represented with error bars in the LP and the DP groups. * significantly different from pre-treatment in the LP group ($P < .05$).

3. Results

Table 1 shows the demographic data of the three groups. There were no significant differences in age, weight, and pre-treatment values regarding pain conditions among the three groups (Table 1).

There were no significant differences in all parameters in the control group. VRS (Figure 3), STAI-I (Figure 4), and MH (Figure 5) values significantly decreased immediately after treatment, and NDI (Figure 6) was lower at 1 day following treatment compared with pre-treatment in the LP and the DP groups. HR (Figure 7) significantly decreased and the HF component of HRV (Figure 9) significantly increased after treatment in the LP group only. There were no differences on the sAA and the LF components (Figure 8) and the LF/HF ratio (Figure 10) of HRV among the three groups. Satisfaction due to acupressure continued to 1 day after the treatment in the LP and the DP groups (Figure 11).

4. Discussion

Our results demonstrated that acupressure on the local and the distal acupuncture points significantly reduced various parameters of the pain-associated conditions, that is, VRS, STAI-I, MH, and NDI whereas there were no significant differences in all parameters in the control group. Although acupressure did not change the LF and the LF/HF ratio of HRV, acupressure on the local acupuncture points significantly reduced HR and increased the HF of HRV. Satisfaction due to acupressure continued until 1 day after treatment on the distal points as well as the local points. These results show that acupressure on not only the local points but also the distal acupuncture points improved pain-related condition, and furthermore acupressure could influence the autonomic nervous system.

Mechanical pressure such as massage and acupressure has been known to decrease tissue adhesion, promote relaxation,

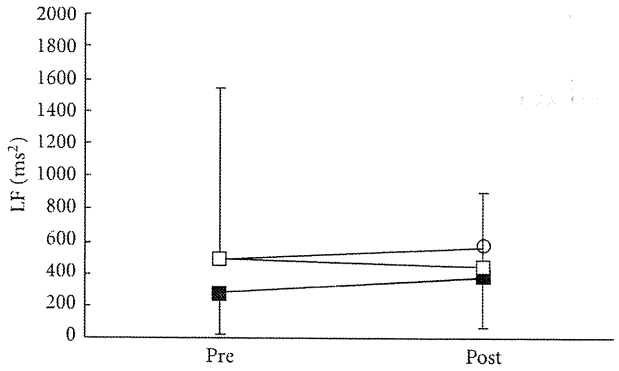

FIGURE 8: Changes in the low-frequency (LF) component of heart rate variability. ○: control group. ■: local acupuncture point (LP) group. □: distal acupuncture point (DP) group. Values are presented as mean. SD represented with error bars in the LP and the DP groups.

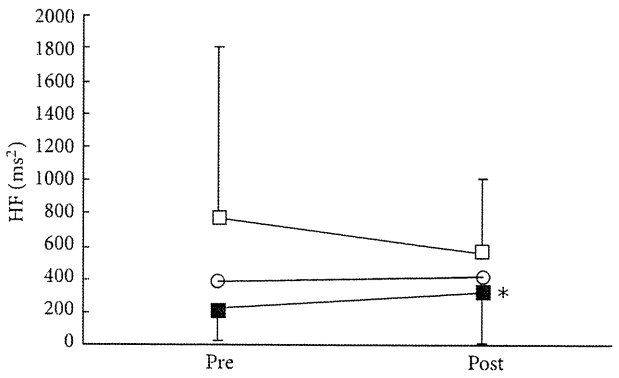

FIGURE 9: Changes in the high-frequency (HF) component of heart rate variability. ○: control group. ■: local acupuncture point (LP) group. □: distal acupuncture point (DP) group. Values are presented as mean. SD represented with error bars in the LP and the DP groups. * significantly different from pre-treatment in the LP group ($P < .05$).

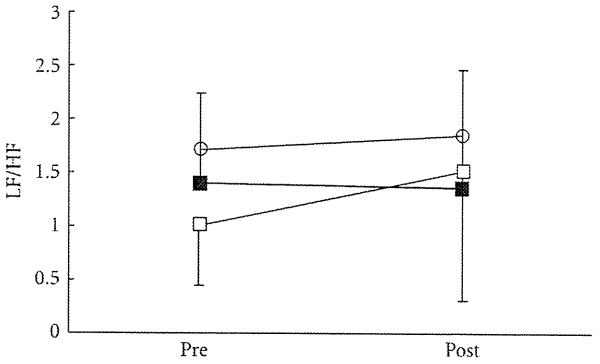

FIGURE 10: Changes in the LF/HF ratio (LF/HF) of heart rate variability. ○: control group. ■: local acupuncture point (LP) group. □: distal acupuncture point (DP) group. Values are presented as mean. SD represented with error bars in the LP and the DP groups.

increase regional blood circulation, increase parasympathetic nervous activity, increase intramuscular temperature, and decrease neuromuscular excitability [15]. Also, many researchers have demonstrated the effect of acupressure and acupuncture for sedation [4, 5, 16, 17].

Acupuncture on the tender points has been commonly used as a treatment for chronic neck pain and appears to alleviate pain and stiffness [1, 18]. The tender points are known to be located at traditional acupuncture points, "*ah si*" point, and also to conform with trigger points and criterion sites for fibromyalgia [1, 18, 19]. Tender points are supposed to be the site where there are nociceptors and polymodal receptors, which have been sensitized by various factors. Thus, stimulation such as acupuncture and acupressure on the tender points may activate sensitized polymodal receptors more powerfully, resulting in stronger effects on pain relief [1]. In traditional acupuncture medicine, tender points eliciting tenderness or pain could be selected when treating chronic neck pain [1].

Acupuncture treatment typically applies to not only the tender points but also the distal acupuncture points for the treatment of chronic pain. Acupuncture at the distal acupuncture points could improve pain conditions in chronic neck pain patients, indicating that nonsegmental antinociceptive systems may play a major role in acupuncture analgesia [2]. Also, electroacupuncture at the acupuncture point "*Hegu*" (LI 4) decreases the activity on anterior cingulated cortex (ACC) and cingulum, thereby inhibiting nociceptive processing in the brain. Acupuncture point stimulation at a rich nerve junction such as "*Hegu*" may reduce pain-induced cingulation processing, thereby resulting in pain relief/analgesia [20]. A study showed that acupuncture improved pain-related disability assessed by NDI [21], as observed in the present study. Furthermore, acupuncture may improve activities at work, the quality of sleep and consequently tiredness, pain-related quality of life, and psychological variables for women with chronic neck pain [22].

Acupuncture has been reported to affect the autonomic nervous system [11, 23]. However, acupuncture/acupressure might have different physiological effects between local and distal acupuncture points, since we showed that acupressure at LI-4, LI-10, and LI-11 did not, but at GB-21, SI-14, and SI-15 significantly influenced autonomic nervous activity.

There are several limitations to the present study. One of them is that we did not perform longer term followup after acupressure. We need further evaluation of the longer effects of acupressure on chronic neck pain and autonomic nervous system. Another limitation is that we showed only the effect of acupressure on either local or distal points. Most acupuncturists and acupressurists use both local and distal points together in clinical practice. Therefore, further study is required in order to assess combinational effects.

In conclusion, acupressure significantly improved pain conditions on not only the local points but also the distal acupuncture points in females with chronic neck pain but affected the autonomic nervous system on only local acupuncture points, as acupuncture points *per se* have different physical effects depending on location.

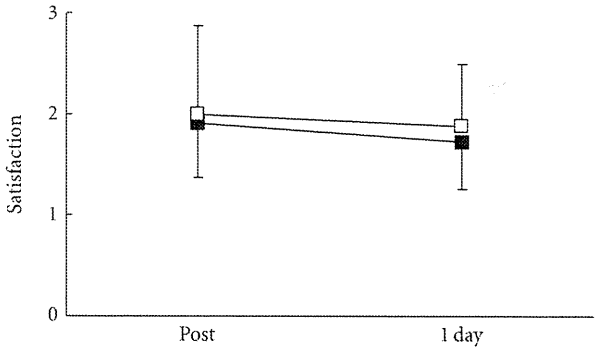

FIGURE 11: Changes in satisfaction due to treatment (VRS: verbal rating scale). ■: local acupuncture point (LP) group. □: distal acupuncture point (DP) group. Values are presented as mean. SD represented with error bars in the LP and the DP groups.

References

[1] S. Jimbo, Y. Atsuta, T. Kobayashi, and T. Matsuno, "Effects of dry needling at tender points for neck pain (Japanese: Katakori): near-infrared spectroscopy for monitoring muscular oxygenation of the trapezius," *Journal of Orthopaedic Science*, vol. 13, no. 2, pp. 101–106, 2008.

[2] D. Irnich, N. Behrens, J. M. Gleditsch et al., "Immediate effects of dry needling and acupuncture at distant points in chronic neck pain: results of a randomized, double-blind, sham-controlled crossover trial," *Pain*, vol. 99, no. 1-2, pp. 83–89, 2002.

[3] J. A. Cambron, J. Dexheimer, P. Coe, and R. Swenson, "Side-effects of massage therapy: a cross-sectional study of 100 clients," *Journal of Alternative and Complementary Medicine*, vol. 13, no. 8, pp. 793–796, 2007.

[4] Y.-C. P. Arai, T. Ushida, T. Osuga et al., "The effect of acupressure at the extra 1 point on subjective and autonomic responses to needle insertion," *Anesthesia and Analgesia*, vol. 107, no. 2, pp. 661–664, 2008.

[5] Y. C. Arai, T. Ushida, T. Matsubara et al., "The influence of acupressure at Extra 1 acupuncture point on the spectral entropy of the EEG and the LF/HF ratio of heart rate variability," *Evidence-Based Complementary and Alternative Medicine*. In press.

[6] K. B. Nilsen, T. Sand, R. H. Westgaard et al., "Autonomic activation and pain in response to low-grade mental stress in fibromyalgia and shoulder/neck pain patients," *European Journal of Pain*, vol. 11, no. 7, pp. 743–755, 2007.

[7] M. Gockel, H. Lindholm, L. Niemistö, and H. Hurri, "Perceived disability but not pain is connected with autonomic nervous function among patients with chronic low back pain," *Journal of Rehabilitation Medicine*, vol. 40, no. 5, pp. 355–358, 2008.

[8] M. Passatore and S. Roatta, "Influence of sympathetic nervous system on sensorimotor function: whiplash associated disorders (WAD) as a model," *European Journal of Applied Physiology*, vol. 98, no. 5, pp. 423–449, 2006.

[9] M. Bäcker, P. Grossman, J. Schneider et al., "Acupuncture in migraine: investigation of autonomic effects," *Clinical Journal of Pain*, vol. 24, no. 2, pp. 106–115, 2008.

[10] V. Johnston, N. L. Jimmieson, G. Jull, and T. Souvlis, "Quantitative sensory measures distinguish office workers with varying levels of neck pain and disability," *Pain*, vol. 137, no. 2, pp. 257–265, 2008.

[11] S. Sakai, E. Hori, K. Umeno, N. Kitabayashi, T. Ono, and H. Nishijo, "Specific acupuncture sensation correlates with EEGs and autonomic changes in human subjects," *Autonomic Neuroscience*, vol. 133, no. 2, pp. 158–169, 2007.

[12] K. Streitberger, J. Steppan, C. Maier, H. Hill, J. Backs, and K. Plaschke, "Effects of verum acupuncture compared to placebo acupuncture on quantitative EEG and heart rate variability in healthy volunteers," *Journal of Alternative and Complementary Medicine*, vol. 14, no. 5, pp. 505–513, 2008.

[13] H. Vernon, "The neck disability index: state-of-the-art, 1991–2008," *Journal of Manipulative and Physiological Therapeutics*, vol. 31, no. 7, pp. 491–502, 2008.

[14] Y.-C. P. Arai, T. Matsubara, K. Shimo et al., "Small correlation between salivary α-amylase activity and pain intensity in patients with cancer pain," *Acta Anaesthesiologica Scandinavica*, vol. 53, no. 3, p. 408, 2009.

[15] P. Weerapong, P. A. Hume, and G. S. Kolt, "The mechanisms of massage and effects on performance, muscle recovery and injury prevention," *Sports Medicine*, vol. 35, no. 3, pp. 235–256, 2005.

[16] S.-M. Wang, D. Gaal, I. Maranets, A. Caldwell-Andrews, and Z. N. Kain, "Acupressure and preoperative parental anxiety: a pilot study," *Anesthesia and Analgesia*, vol. 101, no. 3, pp. 666–669, 2005.

[17] A. Agarwal, R. Ranjan, S. Dhiraaj, A. Lakra, M. Kumar, and U. Singh, "Acupressure for prevention of pre-operative anxiety: a prospective, randomised, placebo controlled study," *Anaesthesia*, vol. 60, no. 10, pp. 978–981, 2005.

[18] T. Nabeta and K. Kawakita, "Relief of chronic neck and shoulder pain by manual acupuncture to tender points—a sham-controlled randomized trial," *Complementary Therapies in Medicine*, vol. 10, no. 4, pp. 217–222, 2002.

[19] M. Bürklein and W. Banzer, "Noninvasive blood flow measurement over acupuncture points (Gb21): a pilot study," *Journal of Alternative and Complementary Medicine*, vol. 13, no. 1, pp. 33–37, 2007.

[20] A. C. N. Chen, F.-J. Liu, L. Wang, and L. Arendt-Nielsen, "Mode and site of acupuncture modulation in the human brain: 3D (124-ch) EEG power spectrum mapping and source imaging," *NeuroImage*, vol. 29, no. 4, pp. 1080–1091, 2006.

[21] L. G. F. Giles and R. Muller, "Chronic spinal pain: a randomized clinical trial comparing medication, acupuncture, and spinal manipulation," *Spine*, vol. 28, no. 14, pp. 1490–1503, 2003.

[22] D. He, A. T. Høstmark, K. B. Veiersted, and J. I. Medbø, "Effect of intensive acupuncture on pain-related social and psychological variables for women with chronic neck and shoulder pain—an RCT with six month and three year follow up," *Acupuncture in Medicine*, vol. 23, no. 2, pp. 52–61, 2005.

[23] E. Haker, H. Egekvist, and P. Bjerring, "Effect of sensory stimulation (acupuncture) on sympathetic and parasympathetic activities in healthy subjects," *Journal of the Autonomic Nervous System*, vol. 79, no. 1, pp. 52–59, 2000.

Alterations of Contralateral Thalamic Perfusion in Neuropathic Pain

Takahiro Ushida*[,1,3], Mitsutaka Fukumoto[2], Carlos Binti[3], Tatsunori Ikemoto[1], Shinichirou Taniguchi, Masahiko Ikeuchi[1], Makoto Nishihara[3] and Toshikazu Tani [1]

[1]*Department of Orthopaedic Surgery, and* [2]*Department of Radiology, Kochi Medical School, Kochi, Japan;* [3]*Multidisciprinary Pain Center, Aichi Medical University, Aichi, Japan*

Abstract: Contralateral thalamus, the place of termination of spinothalamic tract, is affected in patients with pain. We employed single photon emission computed tomography (SPECT) to evaluate the thalamic perfusion in patients with spontaneous neuropathic pain. Ten patients with complex regional pain syndrome (CRPS) and eleven radiculopathiy patients were enrolled in this study. Regional cerebral blood flow of thalamus was assessed bilaterally by iodine-123-labelled iodoamphetamine SPECT. To standardize the inter-patient data, we set a contralateral thalamic uptake index (CTUI) for assessing thalamic asymmetry. In one study, we found elevation of CTUI in patients with symptoms of neuropathic pain for less than 12 month, whereas no change was observed in the case of a longer lasting disease. An another study demonstrated decrease of CTUI after pain treatment, even though it was unrelated to the pain intensity prior to treatment. Our SPECT study revealed that neuropathic pain altered thalamic neuronal activity. CTUIs were increased in early stage of the disease but decreased as the disease progressed to the chronic stage. These results suggest that CTUI can be used to improve management of neuropathic pain for proper evaluation of spontaneous pain.

Keywords: Brain imaging, regional cerebral blood flow, reflex sympathetic dystrophy, pain.

INTRODUCTION

Although neuromuscular disorders are manifested by a variety of clinical symptoms, pain is among those that are particularly hard to endure. Symptoms of pain are believed to have both central and peripheral origin and were studied with the help of neurophysiological and histocytochemical techniques [1, 2]. A number of animal models of spine-related diseases, such as radiculopathy, spinal stenosis, etc., was also introduced to explore the pathways of pain and to examine other related changes [3-5]. These studies were primarily focused on spinal cord due to its accessibility. Limited attention has been paid so far to the brain as well as few studies were undertaken in clinical settings.

In the past decade, several brain imaging techniques, namely single photon emission computed tomography (SPECT), positron emission tomography (PET) and functional MRI (fMRI), emerged as powerful tools used to explore the biology of brain and to diagnose its pathological conditions [6-8]. Since fMRI technology is based on measuring hemodynamic response related to neural activity in the brain, it has advantages in detecting neuroanatomies responded to consecutive functional tasks such as pain stimuli. On the other hand, temporal resolution of SPECT and PET are similarly lower than fMRI technology and beneficial usage of these technologies are rather static brain activation corresponding to spontaneous pain. Although PET enables better resolution, SPECT, is a more affordable and widely used tool. These techniques are informative, noninvasive and extrapolate brain function from changes in the regional cerebral blood flow (rCBF), since it is spatially and temporally coupled to brain activity. Then, three dimensional data are mapped onto the cerebral anatomy.

It was shown that several brain structures, such as bilateral thalamus, insular cortex, cingulate cortex, primary (SI) and secondary (SII) sensory cortex, are activated by noxious cutaneous stimuli in normal subjects [9-13]. Among them, thalamus is viewed as a particularly important one, because spinothalamic tract, a major pathway of pain, terminates into the medial and lateral thalamic nuclei [14]. Clinical studies, however, reported opposite findings. Iadarola *et al.* found significant decrease in thalamic activity contralateral to symptomatic side in PET scans of patients with neuropathic pain [15]. Similar results were obtained for the patients with chronic cancer pain [16]. Therefore, one might assume that changes of contralateral thalamic activity and chronic neuropathic pain are presumably linked. In the present study, we used SPECT to examine whether a relationship exists between contralateral thalamic activity and neuropathic pain in patients with CRPS and radiculopathy.

MATERIALS AND METHODOLOGYS

Subjects

Twenty-one patients with neuropathic pain including ten with complex regional pain syndrome (CRPS) (seven men and three women; aged 27-65 years; time since the onset of

*Address correspondence to this author at the Multidisciplinary Pain Center, Aichi Medical University, 21 Karimata, Yazako, Nagakute, Aichi , Japan; Tel.: + 81 0561-62-5004; Fax: + 81 0561-62-5004;
E-mail: ushidat-koc@umin.ac.jp

1874-4400/10

symptoms 6-34 month) and eleven with either cervical or lumbar radiculopathy (six men and five women; aged 35-74 years; time since the onset of symptoms 0.3-30 month) who agreed with the study protocol were examined. Twenty two healthy volunteers with matching sex and age served as control. All patients had spontaneous pain and sensory impairments only in unilateral upper or lower extremities. Pain status of each patient was evaluated by the visual analogue scale (VAS). rCBF of the contralateral thalamus was assessed by means of Iodine-123-labelled iodoamphetamine single photon emission computed tomography (SPECT). The absence of previous cerebral vascular and psychological diseases was confirmed using brain computed tomography or magnetic resonance imaging by a psychiatrist not involved into the present study.

All protocols were conducted in accordance with the recommendations outlined in the Declarations of Helsinki and were approved by the local Medical Ethical Committee. All subjects signed an informed consent form prior to the examination.

Procedure

SPECT scanning started 10 min after intravenous injection of Iodine-123-labelled iodoamphetamine (111MBq) using an ultra high resolution fanbeam collimators equipped with a triple-detector SPECT device (Toshiba GCA9300A/HG, Tokyo, Japan). Size of field of view used in this study was 409.6mm x 409.6mm. Acquired SPECT images (128 x 128 matrices; 6 mm slice) were transferred to a Windows PC and then reconstructed from projection data by a filtered backprojection technique with Butterworth and Ramp filters according to Talairach brain atlas.

Measurement of CTUI and Image Analysis

Activity of contralateral thalamus was evaluated by calculating the contralateral thalamic uptake index (CTUI). Its measurement consisted of the following steps: a) after setting the identical region of interest (ROI) over the both thalami, rCBF corresponding to it was measured bilaterally; b) thalamic perfusion was standardized by subtracting rCBF of the whole brain to rCBF in ipsilateral and contralateral thalami, respectively; c) CTUI was calculated as the ratio of contralateral to ipsilateral thalamic uptake (Fig. **1A**). ROI was then separated into the medial and lateral subdivisions using the three dimensional stereotaxic ROI template (3DSRT) (Fig. **1B**). Indexes of both subdivisions (CTMUI and CTLUI respectively) were analyzed employing "NIH image" software (developed at the Research Service Branch (RSB) of the National Institute of Mental Health (NIMH), part of the National Institutes of Health (NIH)). Besides, relations between contralateral thalamic uptake index versus disease duration and pain intensity were examined. In controls, the indexes were calculated as the ratio of left to right consecutive thalamic uptakes.

Statistical Analysis

Results were analyzed using Wilcoxon matched pairs and Mann-Whitney tests.

RESULTS

In controls, all CTUI measurements showed symmetric thalamic perfusion (1.17±0.63).

CTUI and Duration of Disease

The most significant increase of CTUI was observed in patients with duration of symptoms of pain for less than 12 months. The average of CTUI was 1.94±1.01, P=0.0166 and in some cases even as high as >3. In contrast, the average of CTUIs in patients with a longer lasting disease (more than 12 month) was similar to controls (1.06 ± 0.45) (Fig. **2**).

Subdivision analysis was resulted no significant change in both CMTUI and CLTUI in patients with duration of disease for more than 12 month compare to controls. Although not statistically significant (P=0.067), an increase

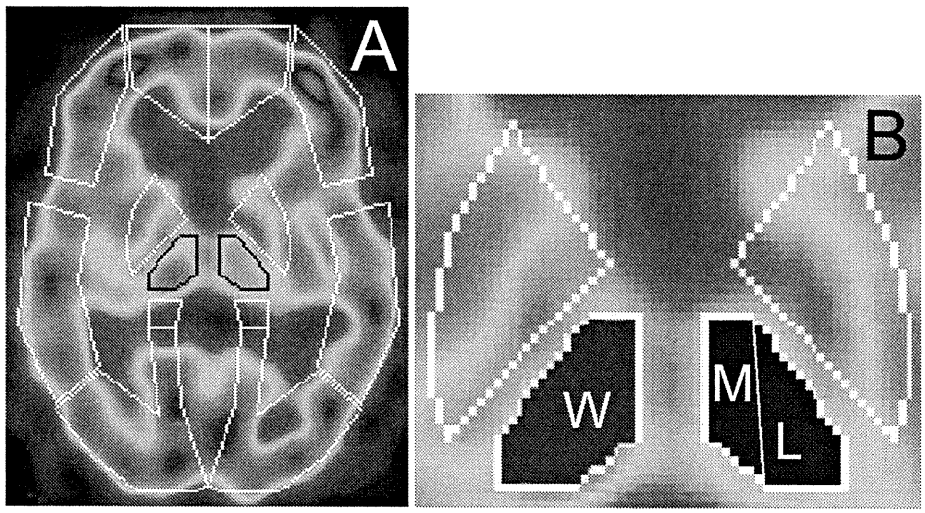

Fig. (1). Standardized brain SPECT images showing presets of ROIs template of 3DSRT (**A**) and subdivisions of thalamus used for CTUI measurements (**B**). ROI over thalami is outlined in black. Whole thalamus is marked as (W), medial and lateral parts as (M) and (L) respectively.

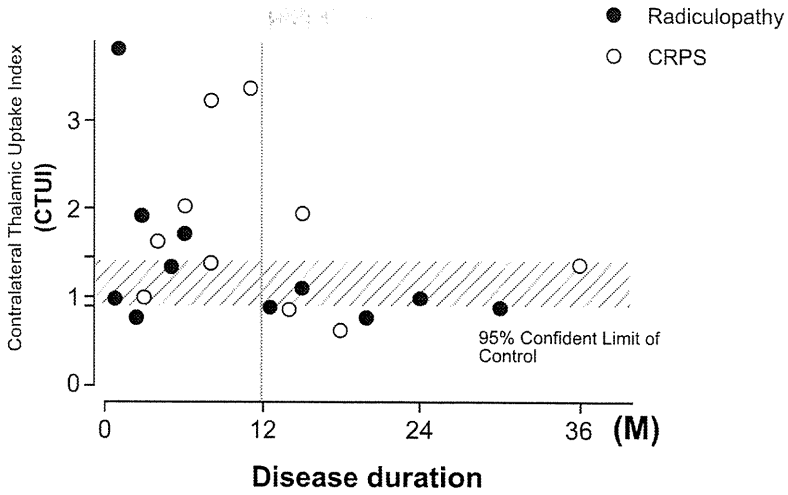

Fig. (2). Scatter gram showing relation between CTUI and disease duration. A significant increase of CTUI is seen for patients with the duration of disease for less than 12 month.

of CMTUI, but not of CLTUI, was observed in patients with duration of disease for less than 12 month (Fig. **3**).

CTUI and Intensity of Pain

In patients with either CRPS or radiculopathy, CTUI and pain intensity, measured by VAS, did not show a clear correlation between each other (VAS=3.5-7.8, average 5,4) (VAS=3.0-7.5, average 4.7), respectively (Fig. **4**).

DISCUSSION

We employed SPECT technique to determine regional concentration of radionuclide in thalamus as a function of time and then to compare its values in normal subjects versus in patients with neuropathic pain. It was observed that contralateral thalamic uptake index (CTUI) is elevated in patients with symptoms of neuropathic pain for less than 12 month. It was also detected that CTUI decreases as a result of pain treatment and that its values in patients with symptoms of pain for more than 12 month are in the range of those in control subjects. This attenuation of the contralateral thalamic activity in chronic pain status has been reported in other investigators. This inhibited thalamic activity might be related to pain pathogenesis, a reversal of this change would be expected as a correlate of pain relief. Accordingly, thalamic hypoactivity has been shown to be reversed by a number of analgesic interventions, from lidocaine blocks to neurosurgical procedures [17-22].

Activation of thalamus in response to acute noxious stimulation as a phenomenon of functional reorganization of central sensory neurons was described previously in both human and animal studies [23-27]. The consensus, however, whether the activation occurs uni- or bi-laterally was not reached. It was also not determined what side of the brain, if uni-laterally, is activated. Our results show that the methodology used to determine thalamic activation by measuring the regional blood flow is of critical importance here. We observed that raw data of thalamic blood flow

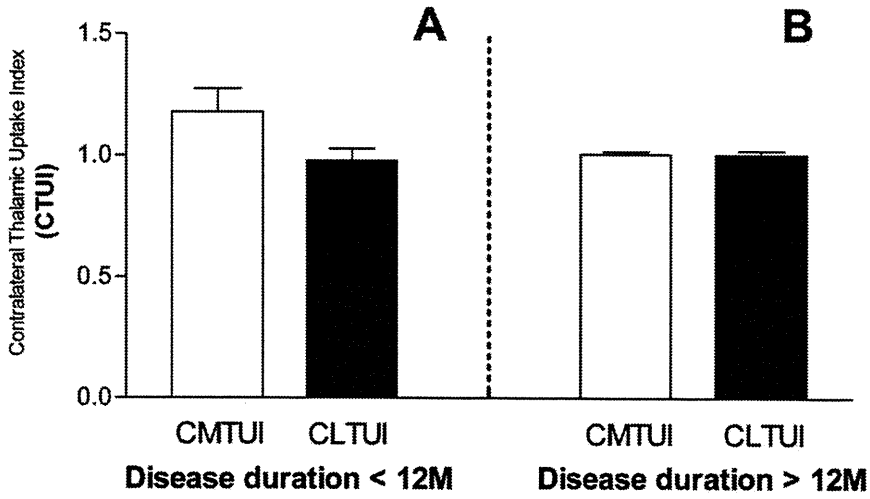

Fig. (3). Changes of CTUI in medial (CMTUI) and lateral (CLTUI) portions of contralateral thalamus in relation to disease duration. An increase of CTUI in medial contralateral thalamus is observed in the case of disease duration for less than 12 month (**A**). No changes between medial and lateral portions are detected in the case of disease duration for longer than 12 month (**B**).

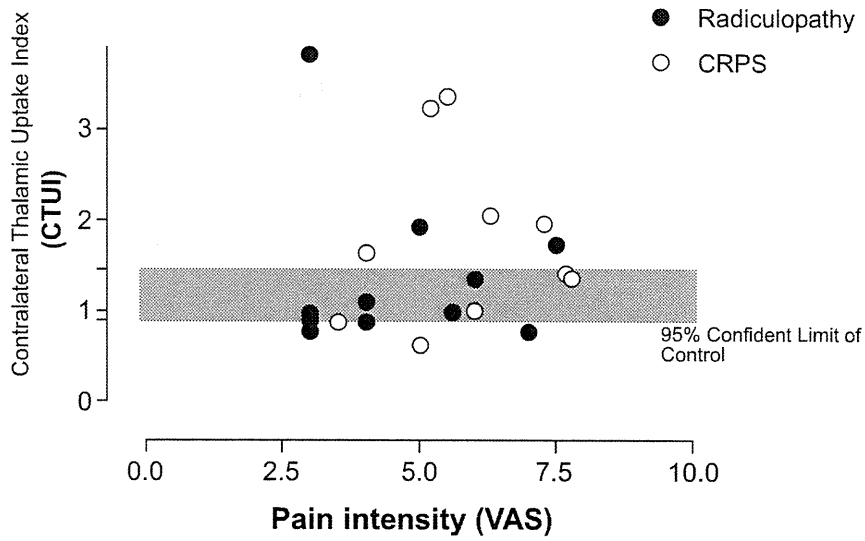

Fig. (4). Scatter gram demonstrating relation between CTUI and pain intensity (VAS). No correlation between pain CTUI and VAS can be found.

obtained from different subjects are not comparable due to significant individual variations. Therefore, we took a different approach and evaluated CTUI by comparing ratios of the total cerebral blood flow against the thalamic blood flow. Using this technique, it was possible to obtain data indicative of an involvement of contralateral thalamus in neuropathic pain. This conclusion is supported by the results of electrophysiological and morphological experiments in primates showing that sensory signals, including noxious inputs, terminate mainly in contralateral thalamus, with less than 10 percent of sensory afferents projecting ipsilaterally [28]. Furthermore, we found an increase of CTUI in the medial portion of contralateral thalamus (CMTUI), but not in the lateral portion, (CLTUI). In this respect, it should be mentioned that medial thalamus is viewed as a portion of thalamus linked to the "affective/motivational" aspect of pain, while lateral is related to "discriminative" pain. Therefore, it is likely that the former aspect of pain sensation is involved the most in patients with neuropathic pain. Additional studies that employ the fine spatial resolution brain imaging tools should help in clarifying this issue further.

Interestingly, we observed that activation of contralateral thalamus depends on the duration of disease and tends to decrease after 12 month since patients report their first complaints. How this observation can be explained? It is possible that sensory cortex adapts to the input of pain in such a way that hyper activation of thalamus for nociceptive transmission and cognition is no longer necessary [29] and /or that continuous pain affects intra-cranial blood distribution and thus results in the sensory blood uncoupling near the activated region [15]. It should be mentioned, however, that the pattern of thalamic reaction in this group of patients is likely to be a very complex issue that requires additional studies considering the possible involvement of other regions of the brain. In recent study, Honda *et al.* [30] focused on to prefrontal area and cingulate area, and found reduction of cerebral blood flow in chronic pain patients as well.

CONCLUSION

We utilized contralateral thalamic uptake index (CTUI) to detect changes of thalamic activity in neuropathic pain. CTUIs were increased in the early stage of the disease but decreased as the disease progressed to the chronic stage. Present results suggest that the activity of contralateral thalamus may have a role in development/maintenance of the chronic pain conditions.

ACKNOWLEDGEMENT

We thank Mr. Naoki Akagi and Mr. Kazuo Morio for technical assistances.

REFERENCES

[1] Tanaka N, Fujimoto Y, An HS, Ikuta Y, Yasuda M. The anatomic relation among the nerve roots, intervertebral foramina, and intervertebral discs of the cervical spine. Spine 2000; 25(3): 286-91.

[2] Heiskari M, Tolonen U, Nystrom SH. Comparison of somatosensory evoked responses from root and cord recorded by skin and epidural electrodes using stimulation of the median nerve in cervical radiculopathy and radiculomyelopathy. Acta Neurochir (Wien) 1986; 79(2-4): 114-9.

[3] Bennett GJ, Xie YK. A peripheral mononeuropathy in rat that produces disorders of pain sensation like those seen in man. Pain 1988; 33(1): 87-107.

[4] Palecek J, Dougherty PM, Kim SH, *et al.* Responses of spinothalamic tract neurons to mechanical and thermal stimuli in an experimental model of peripheral neuropathy in primates. J Neurophysiol 1992; 68(6): 1951-66.

[5] Olmarker K, Holm S, Rosenqvist AL, Rydevik B. Experimental nerve root compression: A model of acute, graded compression of the porcine cauda equina and an analysis of neural and vascular anatomy. Spine 1991; 16(1): 61-9.

[6] Ogawa S, Lee TM, Nayak AS, Glynn P. Oxygenation-sensitive contrast in magnetic resonance image of rodent brain at high magnetic fields. Magn Reson Med 1990; 14(1): 68-78.

[7] Raichle ME, Martin WR, Herscovitch P, Mintun MA, Markham J. Brain blood flow measured with intravenous H2(15)O. II: Implementation and validation. J Nucl Med 1983; 24(9): 790-8.

[8] Apkarian AV, Stea RA, Manglos SH, Szeverenyi NM, King RB, Thomas FD. Persistent pain inhibits contralateral somatosensory cortical activity in humans. Neurosci Lett 1992; 140(2): 141-7.

[9] Derbyshire SW, Jones AK, Gyulai F, Clark S, Townsend D, Firestone LL. Pain processing during three levels of noxious stimulation produces differential patterns of central activity. Pain 1997; 73(3): 431-45.

[10] Derbyshire SW, Jones AK. Cerebral responses to a continual tonic pain stimulus measured using positron emission tomography. Pain 1998; 76(1-2): 127-35.

[11] Coghill RC, Talbot JD, Evans AC, *et al.* Distributed processing of pain and vibration by the human brain. J Neurosci 1994; 14(7): 4095-108.

[12] Casey KL, Minoshima S, Morrow TJ, Koeppe RA. Comparison of human cerebral activation pattern during cutaneous warmth, heat pain, and deep cold pain. J Neurophysiol 1996; 76(1): 571-81.

[13] Casey KL, Minoshima S, Berger KL, Koeppe RA, Morrow TJ, Frey KA. Positron emission tomographic analysis of cerebral structures activated specifically by repetitive noxious heat stimuli. J Neurophysiol 1994; 71(2): 802-7.

[14] Kenshalo DR, Jr, Giesler GJ, Jr, Leonard RB, Willis WD. Responses of neurons in primate ventral posterior lateral nucleus to noxious stimuli. J Neurophysiol 1980; 43(6): 1594-614.

[15] Iadarola MJ, Max MB, Berman KF, *et al.* Unilateral decrease in thalamic activity observed with positron emission tomography in patients with chronic neuropathic pain. Pain 1995; 63(1): 55-64.

[16] Di Piero V, Jones AK, Iannotti F, *et al.* Chronic pain: a PET study of the central effects of percutaneous high cervical cordotomy. Pain 1991; 46(1): 9-12.

[17] Katayama Y, Tsubokawa T, Hirayama T, Kido G, Tsukiyama T, Iio M. Response of regional cerebral blood flow and oxygen metabolism to thalamic stimulation in humans as revealed by positron emission tomography. J Cereb Blood Flow Metab 1986; 6(6): 637-41.

[18] Hsieh JC, Belfrage M, Stone-Elander S, Hansson P, Ingvar M. Central representation of chronic ongoing neuropathic pain studied by positron emission tomography. Pain 1995; 63(2): 225-36.

[19] Peyron R, Garcia-Larrea L, Deiber MP, *et al.* Electrical stimulation of precentral cortical area in the treatment of central pain: electrophysiological and PET study. Pain 1995; 62(3): 275-86.

[20] Pagni CA, Canavero S. Functional thalamic depression in a case of reversible central pain due to a spinal intramedullary cyst: Case report. J Neurosurg 1995; 83(1): 163-5.

[21] Duncan GH, Kupers RC, Marchand S, Villemure JG, Gybels JM, Bushnell MC. Stimulation of human thalamus for pain relief: possible modulatory circuits revealed by positron emission tomography. J Neurophysiol 1998; 80(6): 3326-30.

[22] Garcia-Larrea L, Peyron R, Mertens P, *et al.* Electrical stimulation of motor cortex for pain control: a combined PET-scan and electrophysiological study. Pain 1999; 83(2): 259-73.

[23] Guilbaud G, Benoist JM, Jazat F, Gautron M. Neuronal responsiveness in the ventrobasal thalamic complex of rats with an experimental peripheral mononeuropathy. J Neurophysiol 1990; 64(5): 1537-54.

[24] Rampin O, Morain P. Cortical involvement in dorsal horn cell hyperactivity and abnormal behavior in rats with dorsal root section. Somatosens Res 1987; 4(3): 237-51.

[25] Jones EG, Pons TP. Thalamic and brainstem contributions to large-scale plasticity of primate somatosensory cortex. Science 1998; 282(5391): 1121-5.

[26] Pons TP, Garraghty PE, Ommaya AK, Kaas JH, Taub E, Mishkin M. Massive cortical reorganization after sensory deafferentation in adult macaques. Science 1991; 252(5014): 1857-60.

[27] Florence SL, Jain N, Pospichal MW, Beck PD, Sly DL, Kaas JH. Central reorganization of sensory pathways following peripheral nerve regeneration in fetal monkeys. Nature 1996 ; 381(6577): 69-71.

[28] Willis WD, Kenshalo DR, Jr, Leonard RB. The cells of origin of the primate spinothalamic tract. J Comp Neurol 1979; 188(4): 543-73.

[29] Van Horn JD, Gold JM, Esposito G, *et al.* Changing patterns of brain activation during maze learning. Brain Res 1998; 793(1-2): 29-38.

[30] Honda T, Maruta T, Takahashi K. Brain perfusion abnormality in patients with chronic pain. Keio J Med 2007; 56(2): 48-52.

Received: May 18, 2009 Revised: December 15, 2009 Accepted: February 12, 2010

SPINE Volume 34, Number 26, pp 2848–2857

Tumor Necrosis Factor-Alpha and Its Receptors Contribute to Apoptosis of Oligodendrocytes in the Spinal Cord of Spinal Hyperostotic Mouse (*twy/twy*) Sustaining Chronic Mechanical Compression

Tomoo Inukai, MD, Kenzo Uchida, MD, PhD, Hideaki Nakajima, MD, PhD, Takafumi Yayama, MD, PhD, Shigeru Kobayashi, MD, PhD, Erisa S. Mwaka, MD, MMed, Alexander Rodriguez Guerrero, MD, and Hisatoshi Baba, MD, PhD

Study Design. To examine the distribution of apoptotic cells and expression of tumor necrosis factor (TNF)-α and its receptors in the spinal hyperostotic mouse (*twy/twy*) with chronic cord compression using immunohistochemical methods.

Objective. To study the mechanisms of apoptosis, particularly in oligodendrocytes, which could contribute to degenerative change and demyelination in chronic mechanical cord compression.

Summary of Background Data. TNF-α acts as an external signal initiating apoptosis in neurons and oligodendrocytes after spinal cord injury. Chronic spinal cord compression caused neuronal loss, myelin destruction, and axonal degeneration. However, the biologic mechanisms of apoptosis in chronically compressed spinal cord remain unclear.

Methods. The cervical spinal cord of 34 twy mice aged 20 to 24 weeks and 11 control animals were examined. The apoptotic cells were detected by the terminal deoxynucleotidyl transferase (TdT)-mediated dUTP-biotin nick end labeling (TUNEL) staining. The expression and the localization of TNF-α, TNF receptor 1 (TNFR1), and TNF receptor 2 (TNFR2) were examined using immunoblot and immnohistochemical analysis.

Results. The number of TUNEL-positive cells in the white matter increased with the severity of compression, which was further increased bilaterally in the white matter of *twy/twy* mice. Double immunofluorescence staining showed that the number of cells positive for TUNEL and RIP, a marker of oligodendrocytes, increased in the white matter with increased severity of cord compression. Immunoblot analysis demonstrated overexpression of TNF-α, TNFR1, and TNFR2 in severe compression. The expression of TNF-α appeared in local cells including microglia while that of TNFR1 and TNFR2 was noted in apoptotic oligodendrocytes.

Conclusion. Our results suggested that the proportion of apoptotic oligodendrocytes, causing spongy axonal degeneration and demyelination, correlated with the magnitude of cord compression and that overexpression of TNF-α, TNFR1, and TNFR2 seems to participate in apoptosis of such cells in the chronically compressed spinal cord.

Key words: apoptosis, oligodendrocytes, tumor necrosis factor (TNF)-α, spinal cord, spinal hyperostotic mouse (*twy/twy*), chronic compression. **Spine 2009;34:2848–2857**

Mechanical stimuli applied to the spinal cord can potentially induce profound and irreversible motor paresis secondary to dysfunction and loss of neurons. In particular, long-term and chronic mechanical compression of the spinal cord could gradually cause various pathologic changes of the neural tissue, such as reduced activity of surviving neuronal cells, neuronal degeneration, and demyelination of axons. A number of cadaver studies have examined the pathologic changes in chronically compressed spinal cords of patients with cervical spondylosis or ossified posterior longitudinal ligament showed demyelination as well as loss of axons in the white matter, and loss of neurons in gray matter.[1–3] However, the mechanism responsible for these pathologic changes remains elusive, partly because it is difficult to estimate these changes in human and animal experimental settings and there are few suitable animal models with progressive cord damage induced by long-term compression.

In a series of studies,[4–10] we examined this issue experimentally using the tiptoe-walking Yoshimura (*twy/twy*) mouse, a unique animal that develops spontaneous spinal cord compression. The *twy/twy* mouse is thus suitable for investigating the effects of chronic mechanical compression of the spinal cord, produced without any artificial manipulation of the cord.[4,11] Using these mice, we reported previously a progressive reduction in the number of anterior horn cells when the transverse remnant area of the spinal cord decreased to ≤70% of the control,[4,5] decreased usage of neurotrophins in autocrine and paracrine interactions,[6,8] and presence of accidental and apoptotic dying spinal cord cells.[12] However, the

From the Department of Orthopaedics and Rehabilitation Medicine, The University of Fukui, Fukui, Japan.
Acknowledgment date: February 18, 2009. Acceptance date: May 3, 2009.
The manuscript submitted does not contain information about medical device(s)/drug(s).
No funds were received in support of this work. No benefits in any form have been or will be received from a commercial party related directly or indirectly to the subject of this manuscript.
Supported, in part, by Grant-in-Aid to HB, HN and KU for General Scientific Research of the Ministry of Education, Science and Culture of Japan (grants numbers C15591571, B16390435, B18390411, and B19791023). This work was also supported in part by grants to HB from the Investigation Committee on Ossification of the Spinal ligaments, the Public Health Bureau of the Japanese Ministry of Labor, Health and Welfare (2005–2008).
The authors T.I. and K.U. have contributed equally to this work.
Address correspondence and reprint requests to Kenzo Uchida, MD, PhD, Department of Orthopaedics and Rehabilitation Medicine, The University of Fukui, Matsuoka Shimoaizuki 23–3, Eiheiji, Fukui 910-1193, Japan; E-mail: kuchida@u-fukui.ac.jp

correlation between spinal cord damage and neural cell apoptosis is not fully understood.[9]

Apoptosis of neural cells is an important tissue reaction that contributes to secondary damage after acute spinal cord injury.[13–17] There is evidence to suggest that tumor necrosis factor (TNF)-α can potentially trigger neural cell injury in the spinal cord.[18–20] TNF-α mediates several biologic and immunoregulatory responses in a variety of inflammatory diseases and trauma of the central nervous system,[21,22] including the spinal cord.[23,24] It is highly possible that both TNF receptor 1 (TNFR1) and TNF receptor 2 (TNFR2), which are members of the TNFR superfamily,[25,26] are involved in the cellular reactions mediated by TNF-α. It is highly possible that glial cells may also respond to neuronal cell death in *twy/twy* mouse, but this issue remains totally unknown.

The present study was thus designed to investigate the topographic distribution of glial cell apoptosis, particularly oligodendrocytes, within the chronically compressed *twy/twy* mouse spinal cord as well as the potential role of TNF-α, TNFR1, and TNFR2-mediated cell death cascade. The current communication is the first to describe the potential influence of apoptosis mediated through the TNF-α/TNFR pathway on chronically compressed spinal cord.

■ Materials and Methods

Animal Model

The present series of experiments were conducted in a total of 34 *twy/twy* mice (Central Institute for Experimental Animals, Kawasaki, Japan), aged 24 to 26 weeks with a mean body weight of 29.5 ± 7.3 g (±SD). Mutant *twy/twy* mice were maintained by brother-sister mating of heterozygous Institute of Cancer Research (ICR) mice (+/twy). The disorder is inherited in an autosomal recessive manner and the homozygous hyperostotic mouse is identified by a characteristic tip-toe walking at 6 to 8 weeks of age, although no congenital neurologic abnormalities are detected at that age. The *twy/twy* mouse exhibits spontaneous calcified deposits posteriorly at the C1–C2 vertebral level, producing a variable degree of compression of the spinal cord between C2 and C3 segments (Figure 1A). The calcified mass grows progressively with age particularly in the atlantoaxial membrane, causing profound motor paresis later in life. ICR mice, age-matched with the *twy/twy* mice, were used as controls. Table 1 summarizes the number of mice used in the study. The experimental protocol was approved by the Ethics Committee for Animal Experimentation of our University.

To assess the effect of compression in the longitudinal direction, 3 segments of the cervical spinal cord were selected[5,6]; the segment immediately rostral to the compressive lesion between C1 ventral and C2 dorsal roots (rostral site); the site of maximal compression between C2 and C3 dorsal roots (maximally compressed site); and the segment immediately caudal to the compression lesion between C3 and C4 dorsal roots (caudal site). The length from the caudal site to the rostral site of the spinal cord assessed histologically was on average 3150 μm. To assess the effects of various degrees of spinal cord compression, the maximally compressed transverse remnant area of the spinal cord (TRAS) was used as a parameter of the magnitude of external compression. The ratio of the TRAS in the *twy/twy* mouse to that of the control ICR mouse was designated as TRAS%. We defined TRAS% ≤70% as compressed spinal cord in *twy/twy* mice.[4,5] Mice were divided into 2 groups based on the value of TRAS%: moderate compression group (TRAS% between 50% and 70%, Figure 1B); and severe compression group (TRAS% ≤50%, Figure 1C).

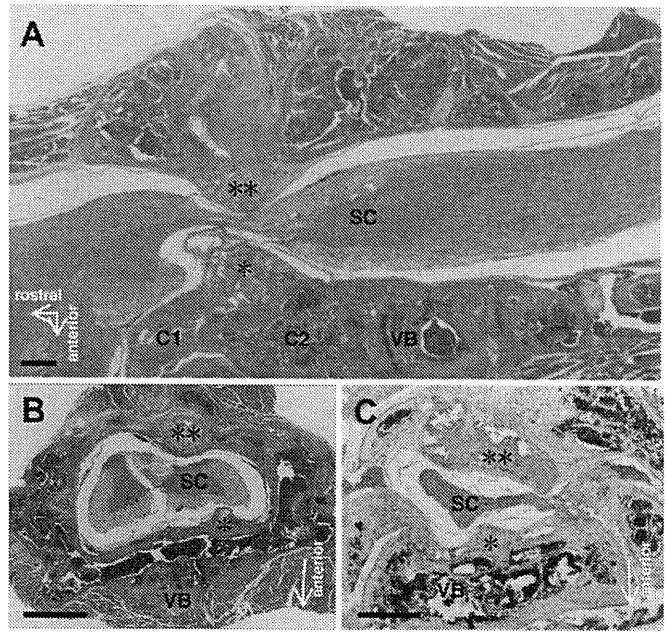

Figure 1. Photomicrographs showing sagittal sections of the spinal cord between the medulla oblongata and C4 spinal cord segment of 24-week-old *twy/twy* mouse (**A**; C1, atlas; C2, axis; Hematoxylin and eosin staining). Calcified lesions (*, **) emanating from the posterior longitudinal ligament and atlantoaxial membrane significantly compress the spinal cord *vis a fronte* (*) and *vis a tergo* (**), respectively. Transverse sections of the spinal cord show moderate compression (**B**) at the maximally compressed site at C1–C2 vertebral levels in 24-week-old mouse and severe compression (**C**) at the same site at the same age. SC indicates spinal cord; VB, vertebral body. Scale bars = 500 μm in (**A**, and 200 μm in **B**, **C**.

Table 1. Number of Mice Used in the Present Study

		twy/twy Mice	
	ICR Mice	Moderate Compression (TRAS% >50% but ≤70%)	Severe Compression (TRAS% ≤50%)
TUNEL staining (paraffin sections)	2	4	4
Electron microscopy	2	2	2
TUNEL and double immunofluorescence staining (frozen sections)	2	4	4
Evaluation of apoptotic signal in oligodendrocytes (frozen sections)	2	4	4
Immunoblot analysis	3	3	3

ICR mice indicates control mice; TRAS, transverse remnant area of the spinal cord.

TUNEL Staining

After anesthesia with intraperitoneal injection of sodium barbiturate (0.05 mg/g body weight), the animal was perfused intracardially using 50 mL phosphate buffered saline (PBS; at 4°C) followed by 100 mL of 4% paraformaldehyde in 0.1 M PBS (pH 7.6). Immediately after perfusion, the cervical cord was removed *en bloc*, postfixed, and then embedded in paraffin. Samples were cut in 4-μm thick serial transverse sections. Deoxyribonucleic acid fragmentation was detected by the terminal deoxynucleotidyl transferase (TdT)-mediated dUTP-biotin nick end labeling (TUNEL) method using the ApopTag Peroxidase In Situ Apoptosis Detection kit (Chemicon International, Temecula, CA). After deparaffinization and hydration, sections were treated with 20 μg/mL of proteinase K in 0.1 mol/L of TRIS buffer (pH 8.0) at room temperature for 15 minutes to strip nuclei of tissue sections. The procedures used were performed as described in the kit manual. The reaction with TdT was terminated by washing the sections with stop-wash buffer for 30 minutes at 37°C. Antidigoxigenin peroxidase was then applied for 30 minutes at room temperature. Color was developed using 3, 3′-diaminobenzidine tetrachloride. Finally, sections were counterstained with methyl green.

Double Immunofluorescence Staining

To identify the type of apoptotic cells, double immunofluorescence staining was performed using frozen sections. The cervical spinal cord was removed as described above and embedded in Tissue-Tek (optimal cutting temperature compound 4583, Sakura FineTechnical, Tokyo) and frozen at −80°C. Serial 25-μm thick transverse frozen sections were treated with 0.1 M TRIS-HCl buffer (pH 7.6) containing 0.3% Triton-X-100 for another 24 hours to allow reaction of the cell membrane with antibodies. Sections were then subjected to TUNEL using an ApopTag Plus Fluorescein *In Situ* Apoptosis Detection kit (Chemicon International). The procedures used were performed exactly as described in the kit manual. The reaction with TdT was terminated by washing the sections with stop-wash buffer for 30 minutes at 37°C. Antidigoxigenin-Fluorescein was applied for 30 minutes at room temperature. After that, the sections were then incubated with antioligodendrocyte monoclonal antibody (RIP, 1:100,000, mouse IgG; Chemicon International) for oligodendrocytes, antineuronal nuclei monoclonal antibody (NeuN, 1:400, mouse IgG; Chemicon International) for neurons, antiglial fibrillary acidic protein monoclonal antibody (GFAP, 1:400, mouse IgG; Chemicon International) for astrocytes, and antimicroglia monoclonal antibody (OX-42, 1:400, mouse IgG; Chemicon International) for microglia diluted in Antibody Diluent with Background Reducing Components (Dako Cytomation, Carpenteria, CA) at 4°C overnight. The sections were then incubated with goat antimouse Alexa Flour 568/fluorescein-conjugated antibody (1:250; Molecular Probes, Eugene, OR). The immunostained cells were visualized under confocal microscope equipped with a 15-mWatt crypton argon laser (model TCS SP2, Leica Instruments, Nusslosh, Germany). The 488- and 543-nm lines of an argon/helium-neon laser were used for fluorescence excitation.

To determine the relationship between TNF-α/TNFR combination pathway and apoptosis of oligodendrocytes in *twy/twy* mice, double staining was performed in a manner similar to that described above. Serial 25-μm thick transverse frozen sections were incubated overnight with OX-42 (1:400, mouse IgG; Chemicon International), GFAP (1:400, mouse IgG; Chemicon International), RIP (1:100,000, mouse IgG; Chemicon International), anti-TNF-α (1:100, gout IgG; Santa Cruz Biotechnology, Santa Cruz, CA), anti-TNFR1 (1:100, rabbit IgG; Santa Cruz Biotechnology), anti-TNFR2 (1:100, rabbit IgG; Santa Cruz Biotechnology), and antiactive caspase-3 (1:100, rabbit IgG; Chemicon International) diluted in antibody diluent with background reducing components (Dako Cytomation) at 4°C. The secondary antibodies were goat antimouse Alexa Flour 568/fluorescein-conjugated antibody (1:250; Molecular Probes, Eugene, OR), donkey antigout antibody Alexa Flour 488/fluorescein-conjugated antibody (1:250; Molecular Probes), and goat antirabbit antibody Alexa Flour 488/fluorescein-conjugated antibody (1:250; Molecular Probes). The immunostained cells were visualized under a confocal laser scanning microscope (model TCS SP2, Leica Instruments).

Immunoblot Analysis

After cardiac arrest, the cervical spinal cord was immediately removed *en bloc* and stored in liquid nitrogen. The sample was solubilized in RIPA buffer (50 mmol/L pH 7.5 TRIS-HCl, 150 mmol/L NaCl, 1% Triton X-100, 0.5% sodium deoxycholate, 20 μg/mL leupeptine, and 1 mmol/L phenylmethylsulfonylfluoride), homogenized and then stored at −80°C. The protein concentration was analyzed by Bio-Rad DC protein assay kit (No. 500–0116, Bio-Rad Laboratories, Hercules, CA). Laemmli sodium dodecylsulfate buffer samples containing proteins were boiled and subjected to immunoblot analysis. Total protein (80 μg/lane) was subjected to sodium dodecylsulfate polyacrylamide gel (15%) electrophoresis and transferred onto polyvinylidene difluoride membrane (PE Applied Biosystems, Foster city, CA) for 70 minutes in a semidry blot apparatus. The membranes were then washed twice in PBS containing 0.05% Tween 20, and then blocked by 5% skim milk in PBS for 1 hour, subsequently reacted with anti-TNF-α (1:200, rabbit IgG; Santa Cruz Biotechnology), anti-TNFR1 (1:200; Santa Cruz Biotechnology), anti-TNFR2 (1:200; Santa Cruz Biotechnology), and antiactive caspase-3 (1:500; Chemicon International) diluted overnight at 4°C sequentially by antirabbit IgG antibody and avidin-biotinylated peroxidase complex (1:200; Envision System-HRP Labeled Polymer, Dako Cytomation) for 3 hours. After triple washing in PBS, the membrane was sunk in the ECL for 1 minute to take a radiograph film for visualization of peroxidase activity. This immunoblot analysis was described in detail in our previous publications.[8–10]

Transmission Electron Microscopy

The cervical spinal cord including the above-described 3 levels of *twy/twy* mice and the same levels of control ICR mice were fixed with 2.5% glutaraldehyde and 2.5% paraformaldehyde, followed by late-fixation in 1% osmium tetroxide for 2 hours. Fixed specimens were dehydrated in a graded series of alcohol, embedded in epoxy resin and polymerized at 60°C for 2 days. Ultrathin sections were cut by ultramicrotome, stained with uranyl acetate and lead citrate, and examined with a Hitachi H-7650 transmission electron microscope (TEM; Hitachi, Tokyo).

Cell Counts and Statistical Analysis

The number of dark-gray colored TUNEL-positive cells was counted in the anterior, lateral, and posterior columns, as well as anterior and posterior horns at each segment of the cervical spinal cord. Four cross-sections were randomly selected out of 10 to 15 sections from each segment of each mouse (4 *twy/twy* mice at each level of spinal cord compression and 2 ICR mice). Similarity in double immunofluorescence staining, the number

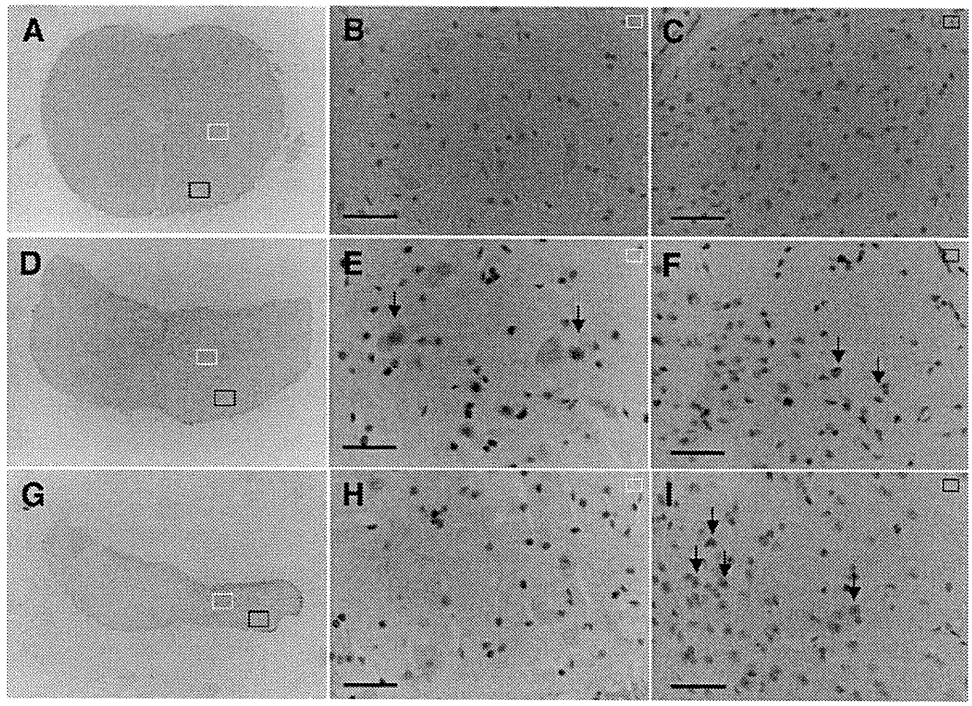

Figure 2. Photomicrographs showing findings of terminal deoxynucleotidyl transferase (TdT)-mediated dUTP nick-end labeling (TUNEL) staining in control ICR (**A–C**) and *twy/twy* (**D–I**) mice. Middle row: spinal cord of a *twy/twy* mouse with a transverse remnant area of the spinal cord (TRAS) of 50% to 70%, bottom row: spinal cord of a *twy/twy* mouse with a TRAS of ≤50%. Left column (**A, D, G**): photomicrographs taken by a roupe (×3). The white rectangular area (anterior horn of the gray matter) and black rectangular area (anterior column of the white matter) are enlarged in the same row in the middle and right columns, respectively. Black arrows: representative TUNEL-positive cells. Scale bars = 50 μm.

of TUNEL- (green) labeled cells and the number of TUNEL- and RIP-(red) double labeled cells (yellow) was counted on the white matter using a fluorescent microscopy. The Mann-Whitney *U* test was used to compare the numbers of TUNEL-positive cells in each region in the moderate and severe compression groups. All values were expressed as mean ± SEM. A $P < 0.05$ denoted the presence of a significant difference between groups.

■ Results

Histologic Evaluation of Apoptosis in the twy/twy Mouse Spinal Cord and Transmission Electron Microscope Findings

Topographic distribution of TUNEL-positive cells in the chronically compressed spinal cord of *twy/twy* mice examined by the TUNEL method is shown in Figure 2. No TUNEL-positive cells were identified in both the gray and white matters of the control ICR mouse spinal cord (Figures 2A–C). In contrast, a number of TUNEL-positive cells were found in the anterior horn (Figure 2E), posterior horn and anterior column (Figure 2F), lateral as well as posterior columns in the *twy/twy* mice with moderate compression (Figures 2D–F). In comparison, fewer TUNEL-positive cells were found in the severe compression group particularly in the anterior horn (Figures 2G, H), though these cells were abundant in the anterior (Figure 2I), lateral and posterior columns.

Figure 3 shows the results of comparative quantitative analysis of TUNEL-positive cells in the posterior and anterior horns, and posterior, lateral and anterior columns at the spinal cord level rostral to compression (Figure 3A), maximal compression (C1–C2 vertebral level, Figure 3B), and caudal to compression (Figure 3C). Fewer such cells were noted in the gray matter at the level of maximal compression (Figure 3B). In the spinal cord

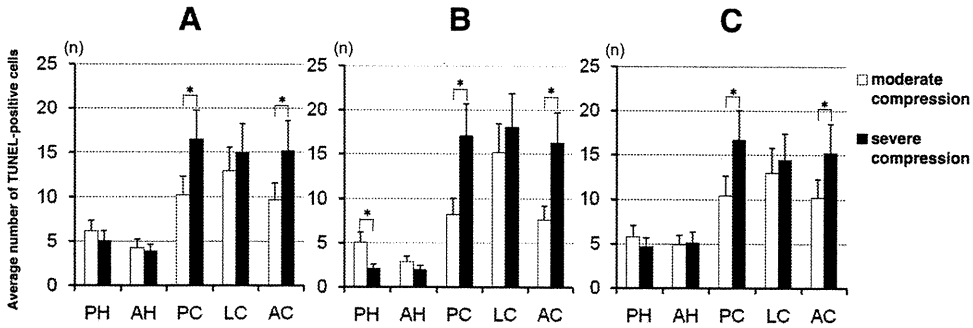

Figure 3. Quantification of distribution of TUNEL-positive cells at 3 representative segments (**A**, site rostral to maximally compressed segment; (**B**,) site of maximal compression at C1–C2 vertebral level; (**C**,) site caudal to the maximal compression) of the *twy/twy* mouse with moderate and severe external compression. Abscissa: representative anatomic site; PH indicates posterior horn; AH, anterior horn; PC, posterior column; LC, lateral column; AC, anterior column of the spinal cord. Ordinate: the number of number of TUNEL-positive cells. The number of TUNEL-positive cells was higher in the white matter (PC, AC) in severe compression compared with moderate compression. There appeared significant decrement in the number of TUNEL-positive cells in the gray matter (PH) in the maximally compressed spinal cord segment (middle graph, **B**). Data are mean ± SEM of number of mice indicated in Table 1. *$P < 0.05$.

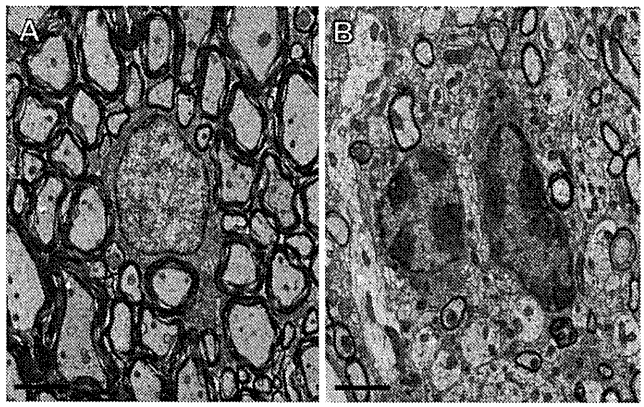

Figure 4. Transmission electron micrographs showing glia-like cells in the white matter of the control ICR mouse (**A**) and *twy/twy* mouse in the maximally compressed spinal cord segment (**B**) with severe compression. The glia-like cell in ICR mouse shows absence of apoptosis (**A**) but in the *twy/twy* mouse, the glia-like cell shows aggregation of nuclear chromatin into dense and sharply delineated masses despite preservation of cytoplasmic organelles, suggestive of cell apoptosis (**B**). Scale bars = 2 μm.

of *twy/twy* mice with severe compression, the number of TUNEL-positive cells was significantly lower in the posterior horn at the segment of maximal compression (Figure 3B), and was also significantly higher in the white matter, particularly, posterior and anterior columns in all 3 spinal cord segments (Figures 3A–C), compared with moderate compression.

TEM examination showed a significant number of apoptotic glia-like cells in the white matter, particularly in the maximally compressed segment of the spinal cord with severe compression. TEM also showed accumulation of nuclear chromatin into dense, finely delineated masses, together with preservation of cytoplasmic organelles (Figure 4B). The presence of TUNEL-positive cells confirmed that these were apoptotic cells. In contrast, no such apoptotic cells were seen in control ICR mice (Figure 4A).

Findings in Double Immunofluorescence Staining

In *twy/twy* mice, most TUNEL-positive cells were also RIP-positive, and the number of TUNEL-RIP double-positive cells appeared to increase with the magnitude of cord compression (Figure 5). The ratio of TUNEL- and RIP-double positive cells to TUNEL-positive cells was on average 59% ± 18% in the moderate compression group and 78% ± 14% in the severe compression group (Figure 5J). A small number of TUNEL-NeuN double-positive neurons were found in moderate and severe compression groups. A few GFAP or OX-42 double-positive cells were identified in some *twy/twy* mice examined with severe spinal cord compression, particularly in the white matter.

TNF-α-Mediated Apoptosis in the twy/twy Mouse Spinal Cord

Next, we evaluated the relationship between TNF-α/TNFR pathway and apoptosis in *twy/twy* mouse spinal cord by immunoblot analysis. Overexpression of TNF-α, TNFR1, and TNFR2, and activation of caspase-3, a marker of apoptosis, was evident in *twy/twy* mouse spinal cord compared with ICR mouse (Figure 6). Semiquantitative immunoblot analysis showed increased immunoreactivity to TNF-α, TNFR1, and TNFR2, and activated-caspase-3, with increase in the magnitude of spinal cord compression.

In *twy/twy* mice with severe cord compression (TRAS% ≤50%), double-staining for TNF-α and OX-42, GFAP and RIP was identified (Figure 7), which was scattered in the compressed cord particularly in the white matter. In sections double-stained for TNFR1, TNFR2, and activated-caspase-3 with RIP, a number of double-stained cells were identified among the abundant oligodendrocytes in the white matter of *twy/twy* mouse with severe cord compression (Figure 8). Expression of TNF-α, TNFR1, TNFR2, and activated-caspase-3 was noted in the abundant oligodendrocytes in *twy/twy* mouse.

■ Discussion

A number of investigators have attempted to characterize the pathologic features of chronically compressed spinal cords of patients with cervical myelopathy secondary to spondylosis or ossified posterior longitudinal ligament.[1–3] These studies reported the presence of exfoliation of anterior horn neurons with progressive spongy degeneration and demyelination in the white matter in areas of spinal cord mechanical compression. In our previous publications, we observed a significant reduction in the number of remaining surviving neurons (Nissl stain-positive motoneurons) when the TRAS% of the *twy/twy* spinal cord decreased to ≤70% of the control.[4,5] Furthermore, we also reported that the extent of demyelination and Wallerian degeneration in the white matter increased proportionately with the magnitude of spinal cord compression.[7] In the present study, we found significant decrement in the number of TUNEL-positive cells in the posterior horn of the gray matter in the maximally compressed spinal cord segment in severe compression. The population of neuronal cells in the posterior horn significantly decreased when the magnitude of external compression to the spinal cord increased at C1–C2 vertebral level,[5] and thus the findings are explained so far as the number of TUNEL-positive neuronal cells at this site also decreased. On the other hand, we found a significant increase in TUNEL-positive cells in the white matter, in spinal cord segments both rostral and caudal to the segment with maximal compression, and that these cells were most noticeable in the anterior and posterior columns of the spinal cords of *twy/twy* mice with severe compression. Although TUNEL staining is not specific to apoptotic cells,[27] because the staining is also positive for necrotic cells, our observation suggests that neuronal loss in anterior horn, after gray matter atrophy or together with spongy degeneration and demyelination in

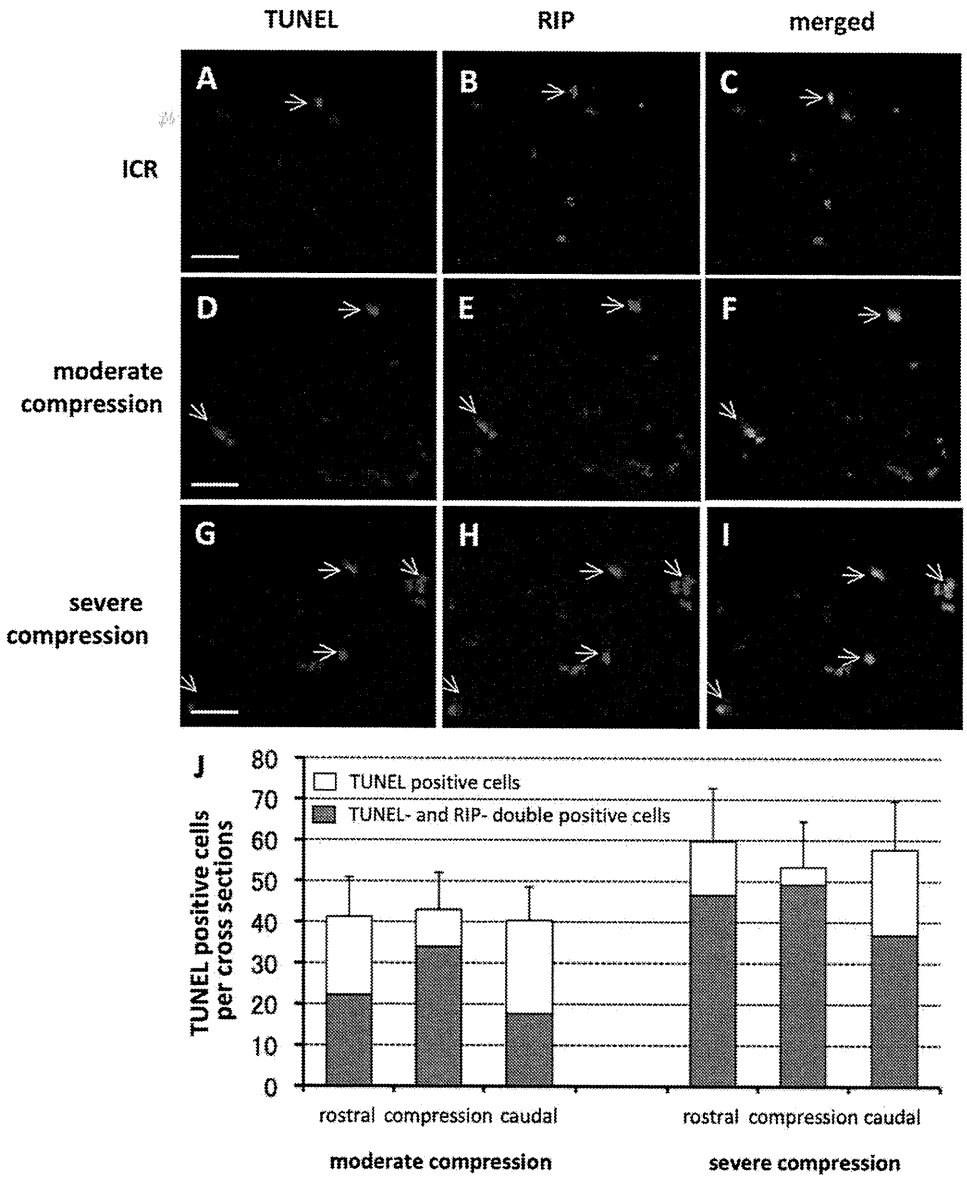

Figure 5. Photomicrographs of double immunofluorescence staining of TUNEL-positive cells with antioligodendrocyte monoclonal antibody (RIP) in the anterior column of the *twy/twy* mouse at maximally compressed C1–C2 spinal cord segment. White arrows in (**A–I**) indicate colocalization of TUNEL and RIP. Overlap of markers appears as yellow color in the middle and bottom rows. Note the increased number of double-stained oligodendrocytes (white arrows) in *twy/twy* mouse with severe compression compared with that of moderate compression. Scale bars = 50 μm. **J**, shows the ratio of TUNEL- and RIP-double positive cells (yellow) to the total number of TUNEL-positive cells (green) in each moderate and severe compression group at 3 representative segments in the white matter (posterior column, lateral column, anterior column). The percentages of TUNEL and RIP double-positive cells out of the total number of TUNEL-positive cells was on average 59% in the moderate compression group and 78% in the severe compression group.

the white matter of the *twy/twy* mouse spinal cord is likely to be due to apoptotic death of neurons and glia.

Apoptosis is an active form of cell death that occurs in a variety of physiologic and pathologic conditions, such as damage to the central nervous system caused by ischemia,[28,29] neuronal degenerative diseases,[30] and viral encephalitis.[31] After spinal cord injury, apoptosis of neurons and glial cells occurs rapidly at the level and vicinity of the traumatic injury, thus contributing to a secondary pathologic cascade of neural injury. Several groups have concluded that neuronal cell apoptosis is the underlying process of spinal cord damage after traumatic injury.[13–15] Our group suggested previously the role of mitogen activated protein-kinase cascade in neuronal cell apoptosis of *twy/twy* mice in addition to other yet unknown mechanism(s).[16] In spinal cord injury, apoptotic oligodendrocytes are found along the spinal cord longitudinal axis both proximally and caudally far from the level of injury, but most significantly at and around the level of injury.[15,17,29] Liu *et al*[15] reported that the initial damage of neurons and oligodendrocytes occurred extensively in the area of direct trauma and that 7 days later, the second wave of injury occurred mainly in the form of apoptotic oligodendrocytes in the white matter proximally and caudally far from the level of direct injury. Several chemical and circulatory disturbances, in addition to other yet unknown mechanisms could contribute to such extensive apoptosis of oligodendrocytes. Crowe *et al*[13] reported that apoptosis of oligodendrocytes occurring distal to the injury site in a spinal cord injury model was possibly due to a lack of neurotrophic factors after axonal damage. It is highly probable for oligodendrocytes and other neural cells to undergo cellular death through this neurotrophin-deficient apoptosis mechanism, and we have reported recently the presence of neurotrophin deficiency-related cell death, including apoptosis, in acute spinal cord injury.[32] Apoptosis of oligodendrocyte correlates significantly with delayed axonal demyelination after spinal cord injury.[29] In the current study in *twy/twy* mouse model, immunocytochemistry of double-stained